Journal of Hydrology 586 (2020) 124887

Contents lists available at ScienceDirect

Journal of Hydrology

journal homepage: www.elsevier.com/locate/jhydrol

Research papers

Monitoring water discharge and floodplain connectivity for the northern Andes utilizing satellite data: A tool for river planning and science-based decision-making

Juan D. Restrepo A[a,*], Albert J. Kettner[b], G. Robert Brakenridge[b]

[a] Department of Earth Sciences, School of Sciences, Universidad EAFIT, AA 3300 Medellín, Colombia
[b] Dartmouth Flood Observatory, Community Surface Dynamics Modelling System, University of Colorado, Boulder, CO, USA

ARTICLE INFO

This manuscript was handled by Emmanouil Anagnostou, Editor-in-Chief

Keywords:
Andes
Magdalena River
Remote sensing
River discharge
Floodplain

ABSTRACT

River discharge data and magnitudes of floods are often not readily available for decision makers of many developing nations, including Colombia. And this while flooding for these regions is often devastating, causing many fatalities and insurmountable damage to the most vulnerable communities. During the wet season, in strong La Niña years, infrastructural damages of over $US 7.2 billion have occurred. Mitigation of such natural disasters lacks data-supported scientific approaches for evaluating river response to extreme climate events. Here, we propose a satellite-based technique to measure river discharge at selected sites for the main northern Andean River, the Magdalena. This method has the advantage of back calculating daily river discharges over a period of two decades, and thus making it possible to calculate return intervals of significant flood events. The study shows that satellite based river discharges well capture a) the inter-annual variability of river discharge; b) the natural seasonality of water discharge along the floodplains; and c) peak discharges that were observed during La Niña conditions between 2008 and 2011. The last is likely more accurate compared to ground-based gauging stations, as ground-based stations tend to overflow during large flood events and as such are hampered to accurately monitor peak discharges. Furthermore, we show that these derived discharges can form the base to study river-floodplain connectivity, providing environmental decision makers with a technique that makes it possible to better monitor river and ecosystem processes.

1. Introduction

Northern Andean rivers have become more vulnerable to floods during recent decades (Restrepo and Escobar, 2018; Restrepo et al., 2018). This as the tropical drainage basins, including the large Magdalena River (Fig. 1), have experienced accelerating deforestation and soil erosion rates during the 1980–2010 period (Restrepo and Syvitski, 2006). The Magdalena River, one of the main suppliers of sediment to the ocean (180 Mt y^{-1}) (Restrepo et al., 2015, 2006; Restrepo and Kjerfve, 2000), has witnessed rising trends in sediment transport during the last three decades. These increasing fluxes correlate well with the observed tendencies in land conversion and deforestation (Restrepo et al., 2015). An important part of the observed increasing sediment flux is being sequestered in riverbeds and along its adjacent floodplains (Kettner et al., 2010; Restrepo and Escobar, 2018), making these Andean rivers less resilient in regulating strong hydrologic pulses during extreme climate events.

In addition to human-induced activities affecting soils, sediment fluxes and the hydrological cycle, the northern Andean basins (Fig. 1B) experience high rainfall rates and associated runoff excess over steep slopes (Restrepo and Syvitski, 2006; Restrepo et al., 2006). Also, the drainage basins are influenced by the El Niño Southern Oscillation (ENSO), which causes dry conditions during the El Niño phase and periods of wet waves during La Niña positive phase. River discharge inter-annual variability is in agreement with the El Niño-La Niña cycle at periods of 3–5 years (Poveda et al., 2001, 2006). Between 2008 and 2011, strong La Niña conditions impacted the northern basins of Colombia and caused economic losses of over $US 7.2 billion (Hoyos et al., 2013).

During La Niña event in 2011, Colombia experienced the strongest floods on record, flooding the country for almost three months by the so called “wet wave” (Hoyos et al., 2013). River authorities and the national disaster office however, lack consistent discharge data for drainage basin planning and flood hazard mitigation (Walschburger et al.,

* Corresponding author.
E-mail address: jdrestre@eafit.edu.co (J.D. Restrepo A).

https://doi.org/10.1016/j.jhydrol.2020.124887
Received 26 November 2019; Received in revised form 20 March 2020; Accepted 22 March 2020
Available online 24 March 2020

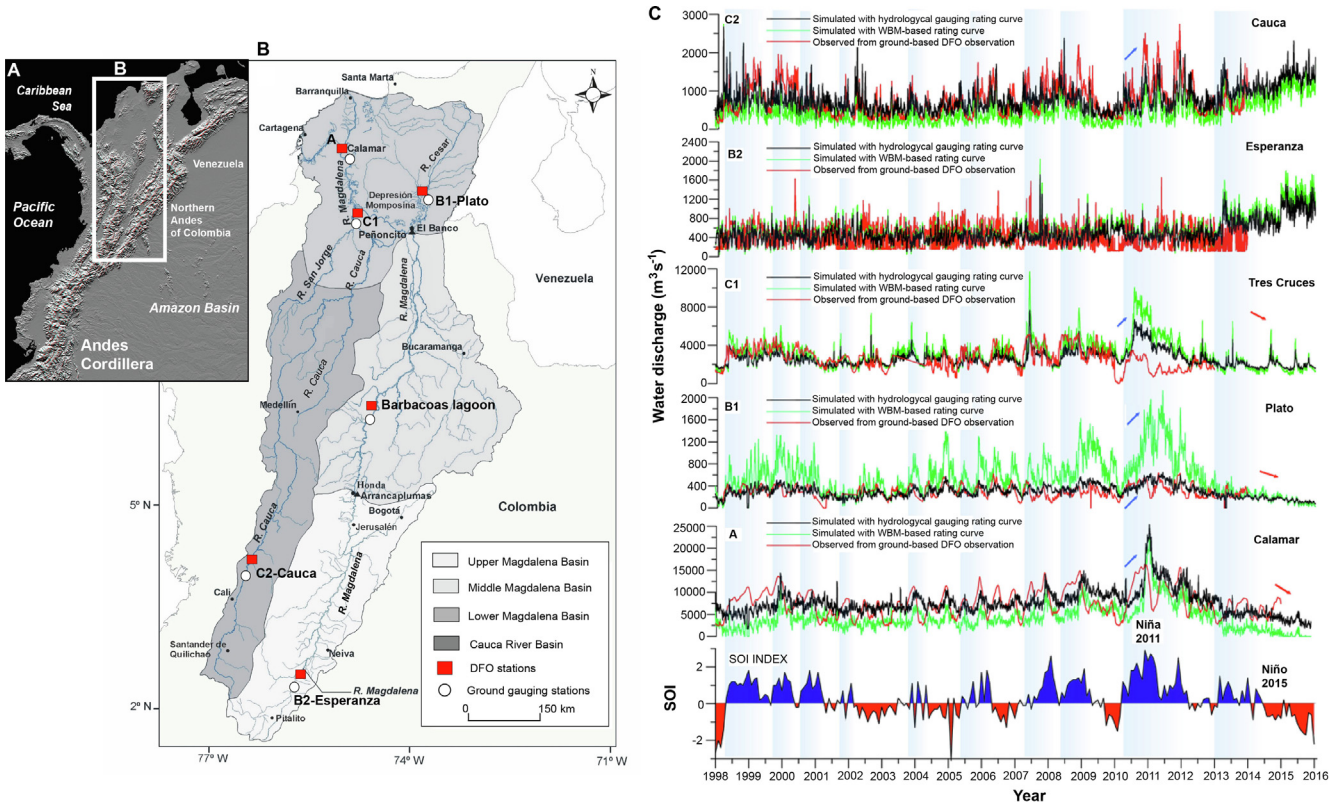

Fig. 1. (A) Northern Andes of Colombia. (B) Ground-based gauging stations and Dartmouth Flood Observatory (DFO) stations used to estimate water discharge and river-floodplain connectivity for the Magdalena River. (C) Water discharge timeseries along the Magdalena River obtained from rating equations utilizing the Water Balance Model (WBM) simulations (green line) and data from hydrological ground gauging stations (black line) (Table 1). The red line shows river flows at each ground-DFO station. We also show the Southern Oscillation Index (SOI) during the 1998–2016 period. (For interpretation of the references to color in this figure legend, the reader is referred to the web version of this article.)

2015). In developing countries like Colombia, the flood alert system is based on records of hydrological gauging stations, which are often poorly calibrated and as such lack accuracy if data is made available at all (Restrepo et al., 2006). River fluxes are underestimated when extreme discharges exceed bank-full discharge. In addition, rating curves are not recalibrated after major floods during La Niña events, resulting in unreliable river discharge magnitudes (Milliman and Farnsworth, 2011).

Water observations in many developing countries are constrained by lack of adequate gauge stations. Many agencies that collect the streamflow or precipitation data are not likely to share this data with others. Thus, the lack of in-situ water data from most of the large river basins of the world implies that we can only use the readily available satellite data sets and global land model outputs. The quasi-global coverage provided by satellite observations combined with open data policies can help avoiding the issues related to data access and continuity (Lakshmi et al., 2018).

For the Magdalena, the best gauged Colombian river (Restrepo et al., 2006), most gauging data are updated and made available for users with a two-year time lag. Therefore, environmental authorities, stakeholders, decision makers, and scientific users do not have access to near-real-time information of river discharge, even when extreme events are unfolding. As such, for many river reaches, satellite-derived discharge estimates offer the only reliable data related to fluvial discharges and flood magnitudes. Therefore, implementing satellite-based tools for near-real-time estimation of river runoff provide support to river planning authorities by making data timely available to scientists and decision makers.

Insufficient and less reliable discharge data also makes it more difficult, if not impossible, to establish river-floodplain hydrologic connectivity relationships. The Momposina depression (Fig. 1B), a significant part of the Magdalena floodplain that covers 10% of the catchment area, is the largest avulsive river system in the northern Andes and consists of the least studied fluvial lakes of major South American Rivers (Latrubesse, 2015; Restrepo and Escobar, 2018). Their ecosystem services provide refuge to aquatic biota and has the capacity to act as a buffer to downstream flooding while supplying potable and irrigation water, and they are recognized as nursery areas for fish species used by artisanal fishery (Jaramillo-Villa et al., 2015). However, ongoing human activities along the whole basin have dramatically changed these vital but fragile ecosystems (Barletta et al., 2010).

According to preliminary environmental assessments, more than 30% of the floodplain lakes along the entire Magdalena River have lost their natural fluvial connection, and many of those lakes as such have diminished or disappeared completely during the last two decades (The Nature Conservancy, 2016). Important questions about the connectivity and hydrological functioning of these floodplains still remain unsolved, including: (1) how has the floodplain morphology changed during the last decades in terms of connectivity with the main river and its flooded areas?; (2) what are the hydrological dynamics of floodplains in terms of recharge water level thresholds?; (3) what are the spatial and temporal dynamics of suspended sediment concentration and how does these processes impact the carbon flux through the food webs in the lakes?; (4) how will hydropower development in the basin change river-floodplain connectivity?; (5) how will the Magdalena navigation project impact floodplain connectivity in the many river reaches in which dredging and course changes are proposed? To answer these questions, it is evident that base-line data is needed, including reliable hydrologic time series to be able to analyze river-floodplain connectivity.

During the last two decades, satellite data have provided spatially and temporally dense river discharge mapping from space (e,g., Alsdorf et al., 2007; Bjerklie et al., 2003, 2005; Brakenridge et al., 1994, 2005,

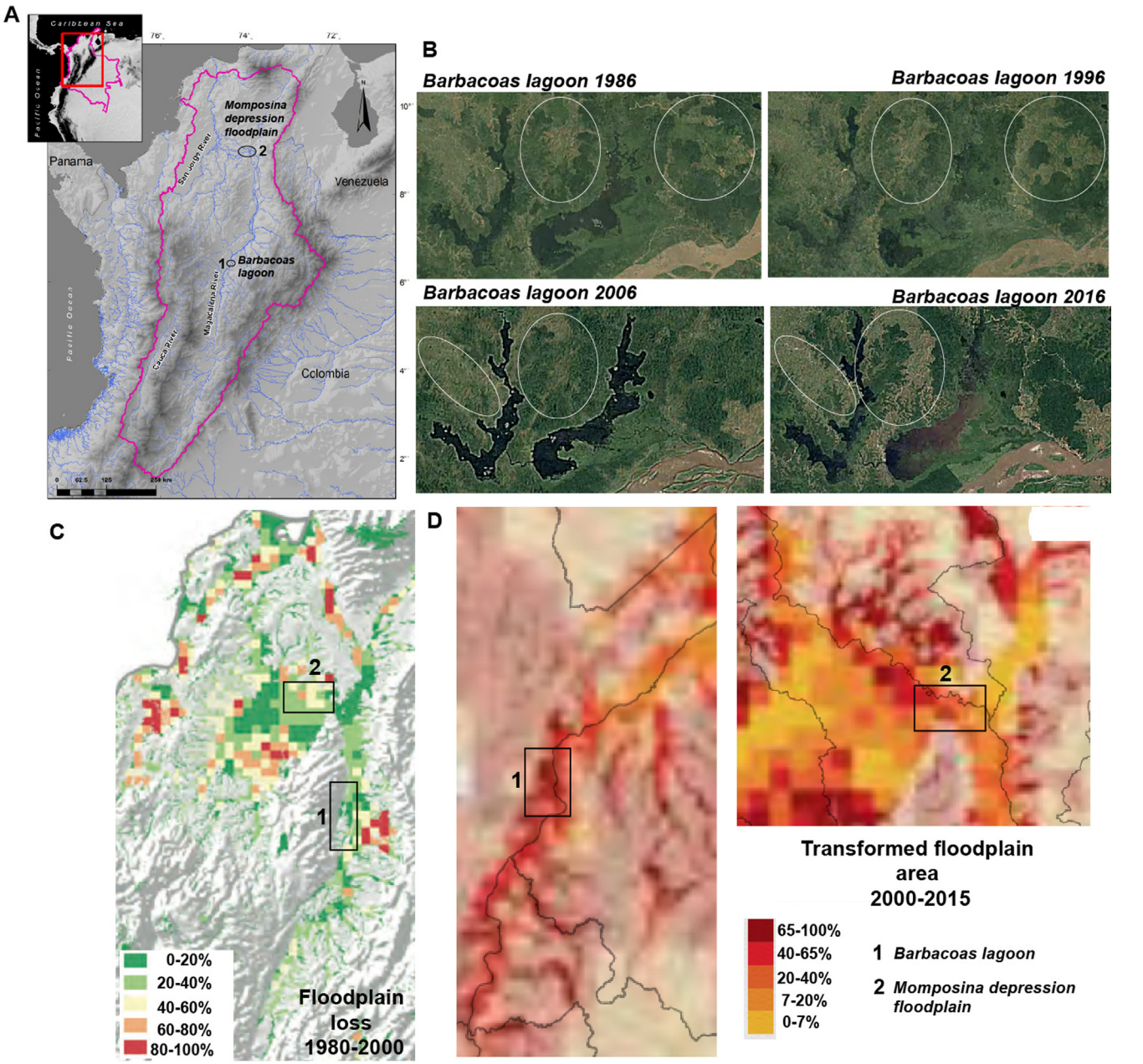

Fig. 2. (A) Magdalena River drainage basin showing the two analyzed floodplain sites, the Barbacoas laggon and the Momposina depression. (B) LandSat images of the Barbacoas lagoon showing areas of deforestation for cattle ranching between 1996 and 2016. (C-D) Assessments of floodplain loss and land transformed area in the Magdalena floodplains (The Nature Conservancy, 2016).

2007; Colin and Smith, 2014; Gleason and Smith, 2014; Koblinsky et al., 1993; Van Dijk et al., 2016). Although these studies highlight the capabilities of satellite data to monitor river discharge, available tools to monitor river flow in real time were not available until recently. The Dartmouth Flood Observatory (DFO) developed the first tools to estimate near-real-time discharge from world-rivers utilizing the Moderate Resolution Imaging Spectro-radiometer (MODIS) in river reaches (Brakenridge et al., 2005). Also, the Advanced Microwave Scanning Radiometer (AMSR-E) was utilized to obtain river flow by monitoring water surface changes along specific 10 km river reaches. These satellite data applications showed that microwave sensors are accurate for monitoring rive with a daily frequency of 1–2 days with the advantage of having low interference from clouds (Brakenridge et al., 2007). Additional work has since explored further general applicability of the approach (Kugler et al., 2019; Van Dijk et al., 2016).

Over the years, DFO has optimized the process of deriving river discharge from satellite data, and can now estimate discharges even for ungagged rivers (Brakenridge et al., 2012; De Groeve et al., 2007), by utilizing a global hydrological model, the global Water Balance Model (WBM) for calibration (Brakenridge et al., 2012). Currently, the Dartmouth Flood Observatory (http://floodobservatory.colorado.edu), River watch version 3.5 measures river discharge in hundreds of reaches along many rivers around the world. To ensure long timeseries of quasi daily data, River Watch stations are based on the passive microwave signals from AMSR-E, AMSR2, TRMM and GPM, processed in collaboration with the Joint Research Centre (JRC) (Brakenridge et al., 2012), allowing to retrieve data from January 1998 onwards (De Groeve et al., 2007).

Northern Andean rivers have become more vulnerable to floods during the last decades. This as land-use changes and deforestation have made these rivers less resilient in buffering strong hydrologic pulses during extreme climatic events. River authorities and flood

Table 1
Mean water discharge values and rating equations obtained from the WBM-based model, ground-based DFO model, and five gauging stations of the Magdalena River. Accuracy statistics, including the DFO R^2 quality levels and signal-noise rating (S/N) are shown (De Groeve et al., 2015). Best regression determination coefficients (r^2) between the satellite signal and WBM and ground-based DFO model simulations are shown after applying 0 and −2 months lags (gray). The *p*-values of the regression between WBM and the ground-based DFO model are also shown.

Site ID	Lat-Long	Channel pattern	a) Mean discharge WBM-based model ($m^3 s^{-1}$)[a]	b) Mean discharge Ground based DFO model ($m^3 s^{-1}$)[b]	c) Mean discharge gauging station ($m^3 s^{-1}$)[c]	d) Gauging station-based equation[d]	R^2	R^2 quality	S/N rating	Accuracy	Lag (months)	d) r^2 WBM-based model	*p* Value	r^2 Ground-based DFO model
A	10.214 −74.924	Moderated anabranching	4420.82	7650.67	7667.71	y = −170,746.49x + 169,553.97	0.32	1	1	1	−2	0.40	0.016	0.22
B1	8.954 −73.934	Avulsive anabranching	5518.63	2963.19	3120.00	y = −28,722.65x + 28,047.70	0.57	2	1.5	1.75	0	0.64	0.0001	0.32
B2	2.744 −75.374	Meandering	549.16	505.87	395.27	y = −34,041.30x + 33,968.17	0.49	2	1	1.5	0	0.37	0.068	0.43
C1	8.594 −74.564	Anabranching	3051.16	2633.93	2642.99	y = −42,939.55x + 44,086.00	0.45	2	2	2	−1	0.47	0.015	0.45
C2	3.824 −76.364	Meandering	485.68	794.04	748.72	y = −89,021.55x + 88,924.22	0.57	2	1	1.5	0	0.48	0.072	0.57

Note: a) River discharge estimates from the Water Balance Model (WBM); b) Water discharge estimates from the ground-based DFO-River Watch microwave signal; c) Water discharge from hydrological gauging stations obtained from Instituto de Hidrología, Meteorología y Estudios Ambientales, IDEAM; d) Transformation of the remote sensing signal to river discharge values is performed using a rating equation. The calibrated discharge values were obtained via rating equations produced in two different ways: 1) via discharge values derived from WBM and 2) via hydrological gauging stations.

mitigation planning lack however, adequate science-supported tools for evaluating river response to extreme climate and human induced events. Here, we use the satellite derived microwave radiometry signal as a tool for estimating near-real-time water discharge for the main northern Andean River, the Magdalena. Stream-flow timeseries during 1998–2016 were obtained and analyzed for six sites along the Magdalena channel for independent and efficient evaluation of discharge variability, flood magnitude estimations and river-floodplain connectivity thresholds. In this study we show that for large, less well-gauged river basins, satellite-based observations are useful for river planners and flood hazard mitigation efforts.

2. Study area

Drainage basins in Colombia are unique Andean fluvial systems due to their geographical setting. Near the Ecuadorian border, the Andes mountain range divides in three parallel branches, the Western, Central, and Eastern Cordilleras (Fig. 1A). Between these Cordilleras lie the Magdalena River, the main fluvial system in the northern Andes and the main contributor of fluvial fluxes into the Caribbean (Fig. 1B) (Restrepo and Kjerfve, 2000). The drainage basin covers 25% of Colombia (258,437 km^2) and hosts nearly 80% of the country's population. The river basin consists of tributary systems with high vertical aggradation, an anastomosing river pattern, and subsiding foreland regions (Latrubesse, 2015). The basin experiences natural erosion processes due to high precipitation rates (annual mean of 2,500 mm), steep slopes exceeding 35°, and strong runoff pulses associated to La Niña events (Restrepo and Syvitski, 2006). All these geomorphic conditions favor high rates of sediment supply and transport from the Andes Cordilleras, making the Magdalena River one of the top ranking world rivers in terms of sediment flux (Restrepo et al., 2015, 2006; Restrepo and Syvitski, 2006).

In addition to natural conditions favoring high rates of sediment yield (Restrepo et al., 2006), human induced impacts such as forest clearance for cattle ranching, agriculture, urbanization and mining, have increased sediment yield rates during the last decades (e.g., Restrepo and Syvitski, 2006; Restrepo et al., 2015). In the Magdalena basin, 80% of the primary forests was cleared by 2000 (Etter et al., 2008) and lowland dry forests were eradicated by 90% (Etter et al., 2006a,b). Therefore not surprisingly, studies of land conversion and sediment transport trends have shown that the magnitude of erosion in the northern Andes has dramatically increased from 500 t km^{-2} y^{-1} to 700 t km^{-2} y^{-1} during the 2000–2010 period, an increase of ~30% (Restrepo et al., 2015).

Human induced changes observed upstream the northern Andean rivers have been also seen downstream along the floodplains (Fig. 2). The floodplains of the Magdalena River, covering 10% of the catchment area, are the largest fluvial fans in the northern Andes and the less well studied fluvial lakes of the major South American Rivers. The floodplains and lakes have important ecosystems services, including: ~50% of the freshwater fishery landings, refuge of aquatic biota, flood control, potable and irrigation water supply, and they are recognized as nursery areas for fish species used by artisan fishery (Jaramillo-Villa et al., 2015). However, the ongoing human activities along the whole basin have dramatically changed these vital ecosystems and fishery landings (Barletta et al., 2010; The Nature Conservancy, 2016). According to some preliminary environmental assessments, more than 30% of the floodplain lakes have lost their natural connections to the main Magdalena River, and many lake systems have diminished considerable or are vanished completely during the last two decades (The Nature Conservancy, 2016) (Fig. 2).

There is no doubt that increasing trends in, and pulses of, upstream sediment transport have made Colombian rivers less resilient to regulate strong hydrologic pulses during extreme climate events. A significant part of the observed increasing fluxes of sediments is becoming sequestered in lakes and or reservoirs, river channels and along the

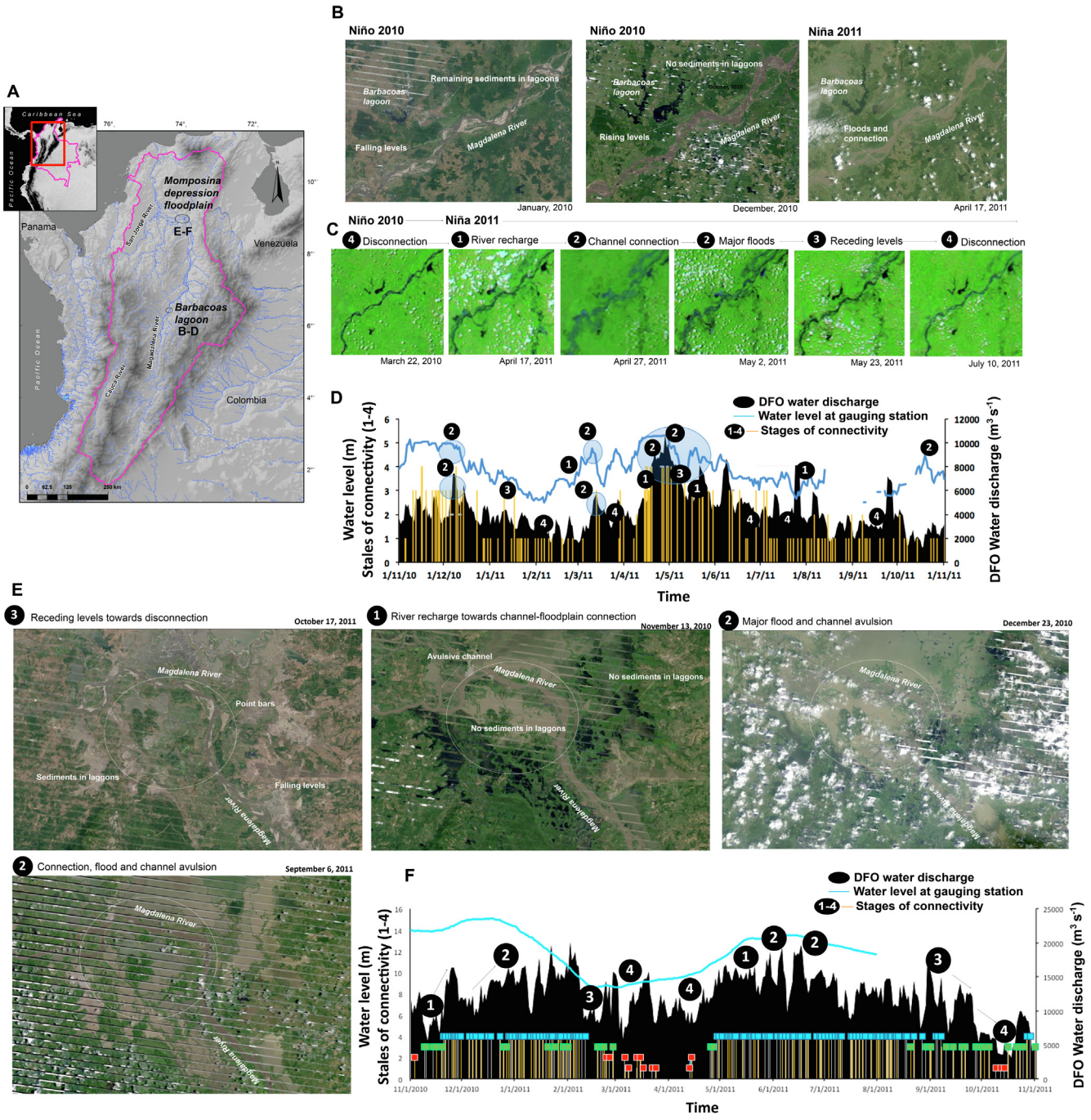

Fig. 3. (A) Magdalena River drainage basin showing the two analyzed floodplain sites, the Barbacoas laggon and the Momposina depression. LandSat (B) and MODIS satellite images (C) showing stages of river-floodplain connectivity for the Barbacoas floodplain during El Niño-La Niña cycle 2010–2011. (D) Time series of satellite-based water discharge, gauged water level, and states of river-floodplain connectivity observed in the Barbacoas lagoon by analyzing daily aqua and terra MODIS satellite images. (E) LandSat satellite images for the Momposina depression showing stages of river-floodplain connectivity. (F) Stages of river-floodplain connectivity for the Momposina depression during 2010–2011.

adjacent floodplains (Kettner et al., 2010; Restrepo and Escobar, 2018). Once the Magdalena River crosses the more flood prune area of the Momposina depression (Figs. 1B and 3), overflow and levee failures will become more common, causing extensive flooding from April until November. At the Momposina depression alone, sedimentation of 3–4 mm y^{-1} over the last 7,500 yr has formed a 130-m-thick deposit (Bray, 2006; Plazas et al., 1988; Smith, 1986). Based on a sediment transport conceptual model, Restrepo et al. (2006) found that 16% of the total annual sediment flux is deposited in the Momposina floodplains alone. Further analysis based on LandSat and MODIS images (Kettner et al., 2010), calculations of sediment load (Restrepo and Escobar, 2018), and sedimentation rates at the downstream Magdalena reaches (Plazas et al., 1988), indicate that approximately 20–80 Mt y^{-1} of sediment is deposited in the Momposina depression floodplains.

All these mentioned environmental facts, including upstream land conversion, deforestation, increasing trends in erosion, and large amounts of sediment trapping downstream, strongly indicate that the Magdalena floodplains are becoming less resilient to floods due to human induced impacts and increasing pulses of sediment flux.

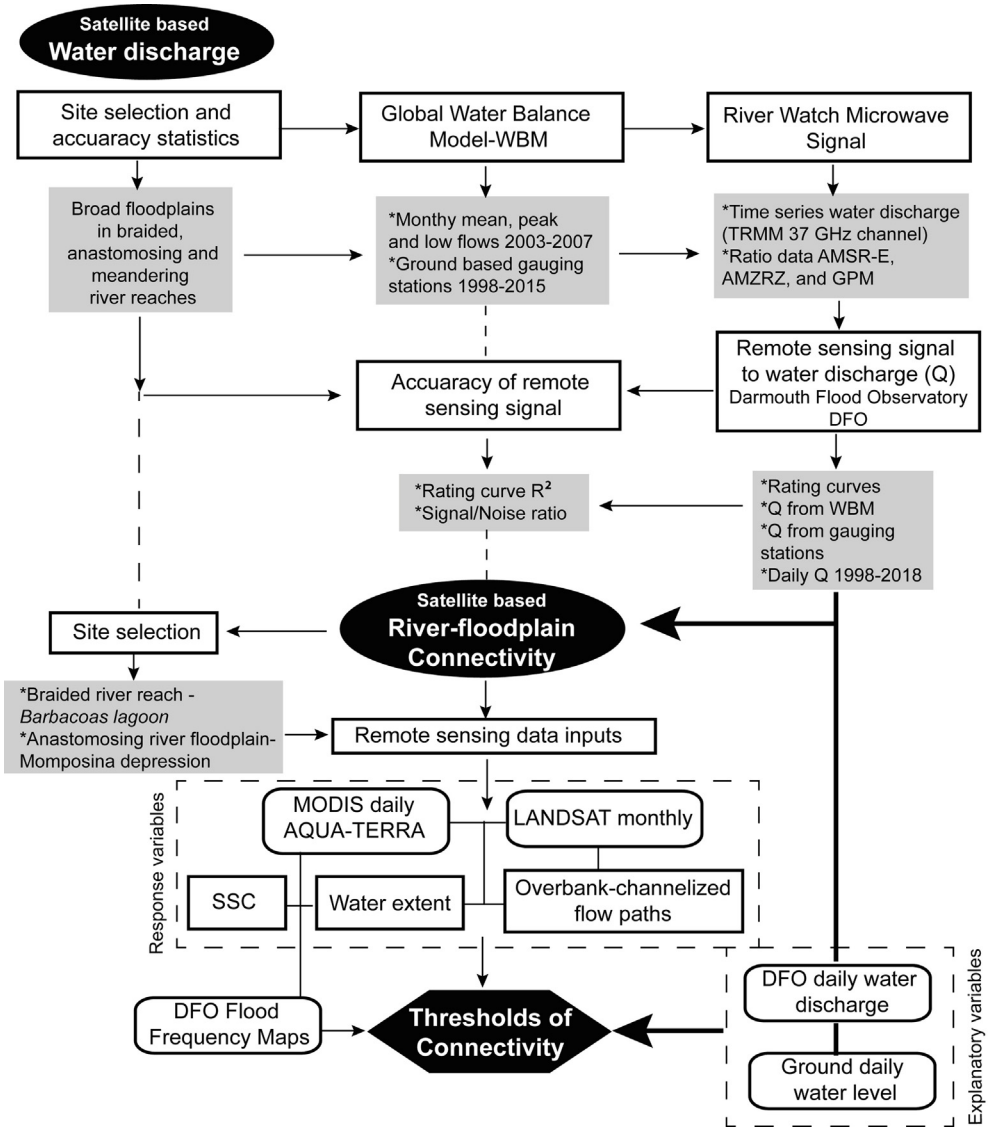

Fig. 4. Scheme of main analyses conducted to estimate water discharge and river-floodplain connectivity using satellite-derived data produced by DFO.

3. Methods

Satellite microwave sensors like TRMM, AMSR-E, AMSR-2, and GPM have a global coverage with a daily return period, and for certain wavelengths the earth surface can be monitored despite cloud cover. Brakenridge et al. (2005) and Van Dijk et al. (2016) showed that by utilizing these sensors, river discharge can be monitored. Applying similar techniques of how discharge is measured on the ground, namely by measuring stage height, variation in the microwave signal reflect changes of river width. So, as water discharge increases, the width of a river increases and therefore the microwave signal changes (Brakenridge et al., 2007, 2012). The microwave data has typically a spatial resolution of 10x10km, which is sufficient, when located over a river, to observe discharge variation over time as long as the area includes both land (high emission) and water surfaces (low emission). The data is inverse in that as water rises (so the area of the water increases) the total emitted radiation reduces as land surface area becomes smaller for that pixel. With the use of the hydrologic model WBM (the Water Balance Model) this microwave signal can be translated into a discharge. Recently, Lakshmi et al. (2018) have demonstrated the application of the satellite-based WBM on estimating available water in the major global river basins. The authors show how the WBM can be used to estimate total water fluctuations and to compare hydrologic spatial and temporal variations across large hydrologic regions. This technique has been applied for many rivers at the Dartmouth Flood Observatory and is made semi-operational through the River Watch 3.5 system (Brakenridge et al., 2012).

For the Magdalena River, six sites (Fig. 1B) were selected for which both satellite-based observations as well as ground based gauged data were obtained. The ground-based gauge data was obtained from the Hydrological and Environmental Institute of Colombia, IDEAM. A simple regression function is normally established between the hydrological modeled data and the satellite microwave data. For this study also a regression function was established by using the ground based gauged data. This to assess the model-based and ground gauged-based rating curves for model bias and accuracy of the Riverwatch System (Brakenridge et al., 2012) (Table 1). Accuracy of rating curves and data from selected hydrological gauging stations were assessed in previous studies along the Magdalena River (e.g., Restrepo et al., 2006; Kettner et al., 2010: Restrepo et al., 2015).

So, to obtain timeseries of satellite-derived water discharge during the 1998–2016 period (Fig. 1C), we used both modeled discharge as observed discharges and: (1) established a rating curve between gauged data and the microwave data to generate daily discharges for the period

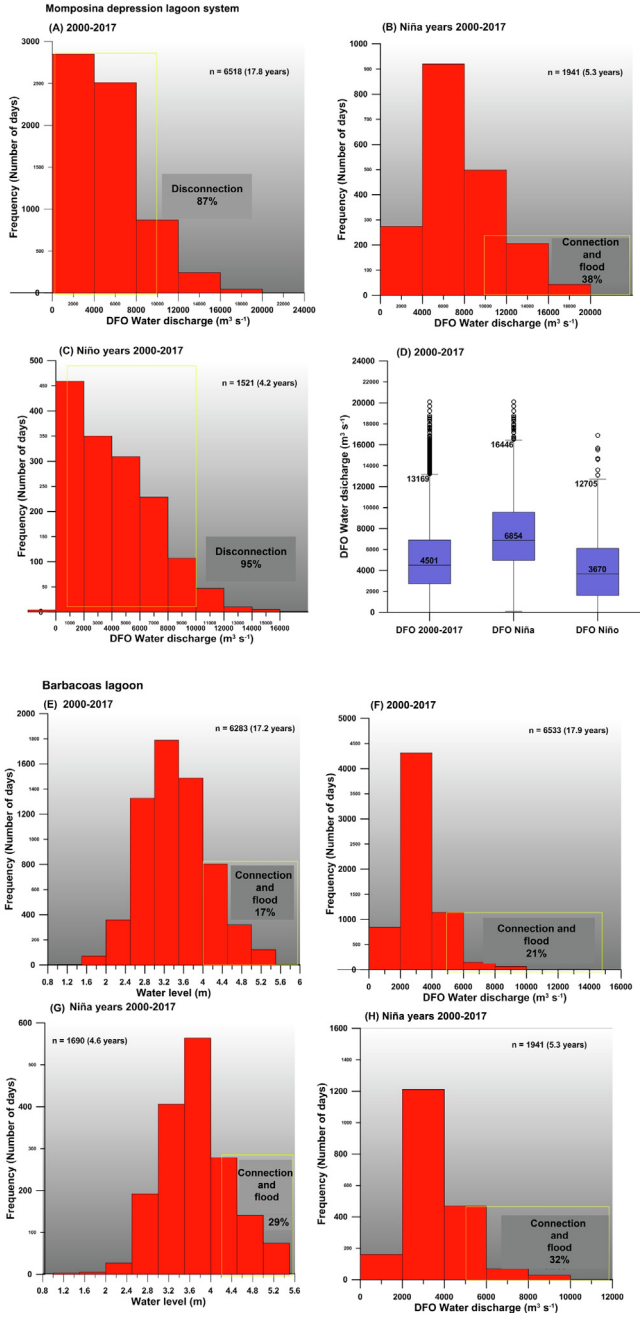

Fig. 5. (A–C) Histograms of estimated satellite-based thresholds of connectivity for the Momposina depression floodplain during the period 2000–2017, including La Niña and El Niño years. The box-whisker plot of satellite-based water discharge during 2000–2007 is also shown (D). (E-H) Histograms of gauged water level and DFO satellite-based thresholds of connectivity for the Barbacoas lagoon during 2000–2017, including La Niña years.

of interest (Table 1), (2) established a rating curve between modeled data and the microwave data to generate daily discharges for the period of interest, (3) applied accuracy assessments and stats on how discharges are performing based on the satellite signal as compared to gauging sites (Table 1), and (4) improved the fitness of the rating curves through calibration equations between gauging station discharge and modeled WBM discharge, after applying different lag times.

To assess the application of satellite-derived water discharge series to identify thresholds of river-floodplain connectivity, we selected two different floodplain sites: the Barbacoas lagoon, a confined floodplain in a meandering river reach, and the Momposina depression system, an avulsive anabranching floodplain (Figs. 1B and 3). Daily near-infrared aqua and true-color terra moderate resolution MODIS satellite images were acquired for the period 2000–2017. Daily images were examined during dry, transition, and wet seasons, as well as during the monsoon (La Niña) and El Niño years. Pixels that over time turn black in the near-infrared MODIS images indicate the extension of floodplain lakes surrounding the Magdalena River and the Momposina region while MODIS true-color terra images were used to visualize sediment spills of the Magdalena River flowing on the floodplains.

In order to establish at what water level and satellite-based water discharge each floodplain starts to flood, we constructed timeseries of different connectivity stages by using MODIS images derived black (low turbidity) and white waters (higher turbid river waters) as indicator. Four stages of connectivity were identified: (1) river recharge (hydrological connection to floodplain as evidenced by floods), (2) channel-connection between river and floodplain (as evidenced by white waters), (3) receding flows towards disconnection, and (4) disconnection (Figs. 3, 5 and 6). According to the identified thresholds of river-lagoon connectivity (Fig. 6), percentages of connection time were calculated from frequency histograms of water level and DFO water discharge series (Fig. 5).

The main methodological steps followed in this study to estimate water discharge and river floodplain connectivity utilizing the microwave data (De Groeve et al., 2015) are shown in Fig. 4.

4. Results

4.1. Satellite timeseries of river discharge

Six stations along the Magdalena and Cauca Rivers were selected for installation of new River Watch measurement sites (or “satellite gauging sites”) (Fig. 1B). Each site is a single 10 km square pixel within a global gridded product developed by the JRC for its “Global Flood Detection System” (GFDS, De Groeve et al., 2015). The morphologies of these river reaches include braided, anastomosing or meandering plane forms and all have distinctive floodplains. Such floodplain units support considerable variations in water surface extension with changes in river flow. The River Watch/GFDS flow area-sensitive signal varies between 0.84 and 0.99 at Calamar (A), while at Plato (B1) the signal varies between 0.72 and 0.96. Other stations, including Tres Cruces, Cauca, and Esperanza, experienced variations between 0.84 and 0.98 (Fig. 7A). This signal is the ratio between emissivity of a pixel that represents the day's driest (the 95th percentile) emissivity within a 9 × 9 pixel array surrounding the emissivity of a selected river – floodplain site. This ratio is used instead of simply the measurement pixel radiance alone in order to remove temporal variation (such as from land temperature) affecting all of the terrain, and isolate the hydrological signal. At the microwave frequency used, increasing in-pixel coverage by surface water as compared to land produces a robust decline in measured radiance, and is much stronger than that observed also by soil moisture changes (Brakenridge et al., 2007).

As expected, sites located in the Momposina depression floodplain, such as Calamar (A), Tres Cruces (C1), and Plato (B1), showed large variability in the signal ratio during the1998-2016 period (Fig. 7A), a condition that indicates high variability in water surface area. In fact, the station at Plato (B1) displays the more accurate microwave signal after WBM calibration. In contrast, upstream stations with limited floodplains, including Esperanza (B2) and Cauca (C2) (Fig. 1B and 7A), showed weaker satellite detection of water surface variability as clearly seen in the smaller variations of the microwave ratio value (Fig. 7A). However, it was later observed that regardless the small variation in the microwave signal, the values of river discharge at these stations were accurate.

We used WBM simulations and data from five hydrological gauging stations to obtain river discharges (Table 1). Linear regressions and determination coefficients (r^2) between ground and simulated river

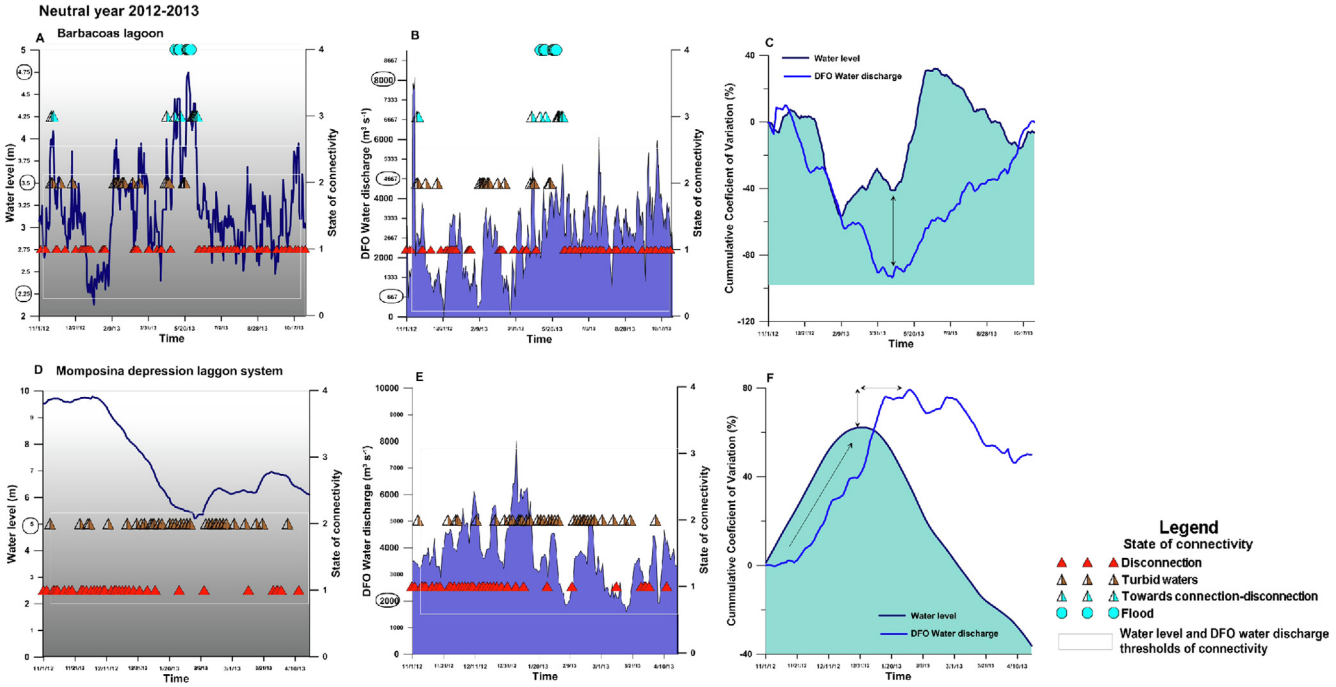

Fig. 6. Examples of timeseries of water level (A, D), satellite derived water discharge (B, E) and coefficient of variation between for water level and satellite derived water discharge (C, F) for the Barbacoas lagoon and the Momposina floodplain during a neutral year 2012–2013. Observed stages of connectivity through MODIS images are superimposed to series in order to define thresholds of connectivity.

discharges were calculated for different time lags (months) (Fig. 7B). Regression fits improved once discharge was lagged by some months. For example, at Calamar, determination coefficient r^2 between satellite data and WBM-river discharge ranged from 0.10 at lag 0 months to 0.40 at a lag of −2 months, indicating that the simulated river flow of the WBM model at this site is too fast. WBM is a global model so such routing speed errors for individual rivers are not surprising. However, results in the Momposina depression floodplain at Plato (B1), show that the satellite signal and WBM river discharge are well correlated with a coefficient r^2 of 0.64 with no lag months (Table 1 and Fig. 7B). In addition, satellite data and river discharge from ground-gauging stations are well correlated with $r^2 = 0.57$ at a lag of −2 months (Fig. 7B). Additional regression fits were performed at stations Tres Cruces (C1), Cauca (C2), and Esperanza (B2) with r^2 coefficients between 0.40 and 0.64 (Table 1 and Fig. 7B).

The rating equations obtained from the WBM-based model, ground-based model, and gauging stations at the analyzed sites (Fig. 1B) were used to convert the satellite signal to water discharge (Table 1). Overall, the inter-annual variability observed at ground gauging stations is followed quite well by satellite-observed river discharges (Fig. 1C). For the stations at Esperanza (B2) and Cauca (C2), the satellite signal captures well the short wave fluctuations, whereas larger variations are observed in the floodplains more downstream at Plato (B1) and Tres Cruces (C1) (Fig. 1C). Here, satellite-observed river discharge follows well the observed discharges at ground gauging stations, especially during high flow conditions. It is worth noting that during peak discharge events, the WBM rating curve overestimates the river discharge magnitudes at Plato (B1) station (Fig. 1C). In general, simulated versus observed river discharges match quite well in the downstream-floodplain stations (Figs. 1C and 7B).

In the upper basin, the satellite site at Esperanza (B2) is located in a narrow channel with limited alluvial plains, downstream two major dams. Here, the satellite signal catches well the short-term fluctuations of observed ground discharges (Fig. 1C). Also, the upstream station at the Cauca tributary (C2) witnessed a good agreement between the satellite river discharges and the observed stream flows (Fig. 1C) despite its location on a constrained river reach with narrow floodplains.

The ENSO cycle is also well captured by the satellite-observed discharge variability (Fig. 1C). During La Niña phase 2010–2011, the magnitudes of measured discharge match well with the Southern Oscillation Index values, whereas low discharge values are observed during El Niño conditions of 2015–2016 (Fig. 1C). However, the upstream Magdalena station at Esperanza (B2) does not exhibit a clear control by the ENSO variability because its river discharge is mainly controlled by the operation of dams.

To evaluate how well time series of satellite-based water discharge capture the observed and measured inter-annual variability related to the ENSO cycle, we used the Continuous Wavelet Transform (CWT) (Fig. 8) (Restrepo et al., 2014; Torrence and Compo, 1998). The CWT function was applied on monthly gauged water discharge and satellite-based discharge at Plato (B1) and used to visualize the periodicities and variability patterns. Clearly, the satellite-based measured discharge properly follows the annual fluctuation as well as the inter-annual variability due to the ENSO oscillation at Plato (B1). The variance spectrum shows that the satellite measured discharge catches significantly better the annual fluctuation and the 2 to 4 years inter-annual variability compared to ground-based gauged river discharge (Fig. 8C, right).

4.2. River-floodplain connectivity thresholds utilizing DFO satellite data

To assess the applicability of satellite derived discharge data on identifying thresholds of river-floodplain connectivity, we selected two different floodplain sites: the Barbacoas lagoon, a confined floodplain system in a meandering river reach, and the Momposina depression, an avulsive, anabranching floodplain (Fig. 1B). Daily near-infrared aqua and true-color terra moderate resolution MODIS satellite images were collected for those areas and analyzed for the period between 2000 and 2016. Satellite based discharge data were downloaded from the DFO River Watch system. Daily images were examined during dry, transition, and wet seasons, as well as during La Niña and El Niño years since 2000. Pixels that over time turn black in the near-infrared MODIS images indicate the extension of floodplain lakes bordering the Magdalena River and the Momposina region, while MODIS terra optical

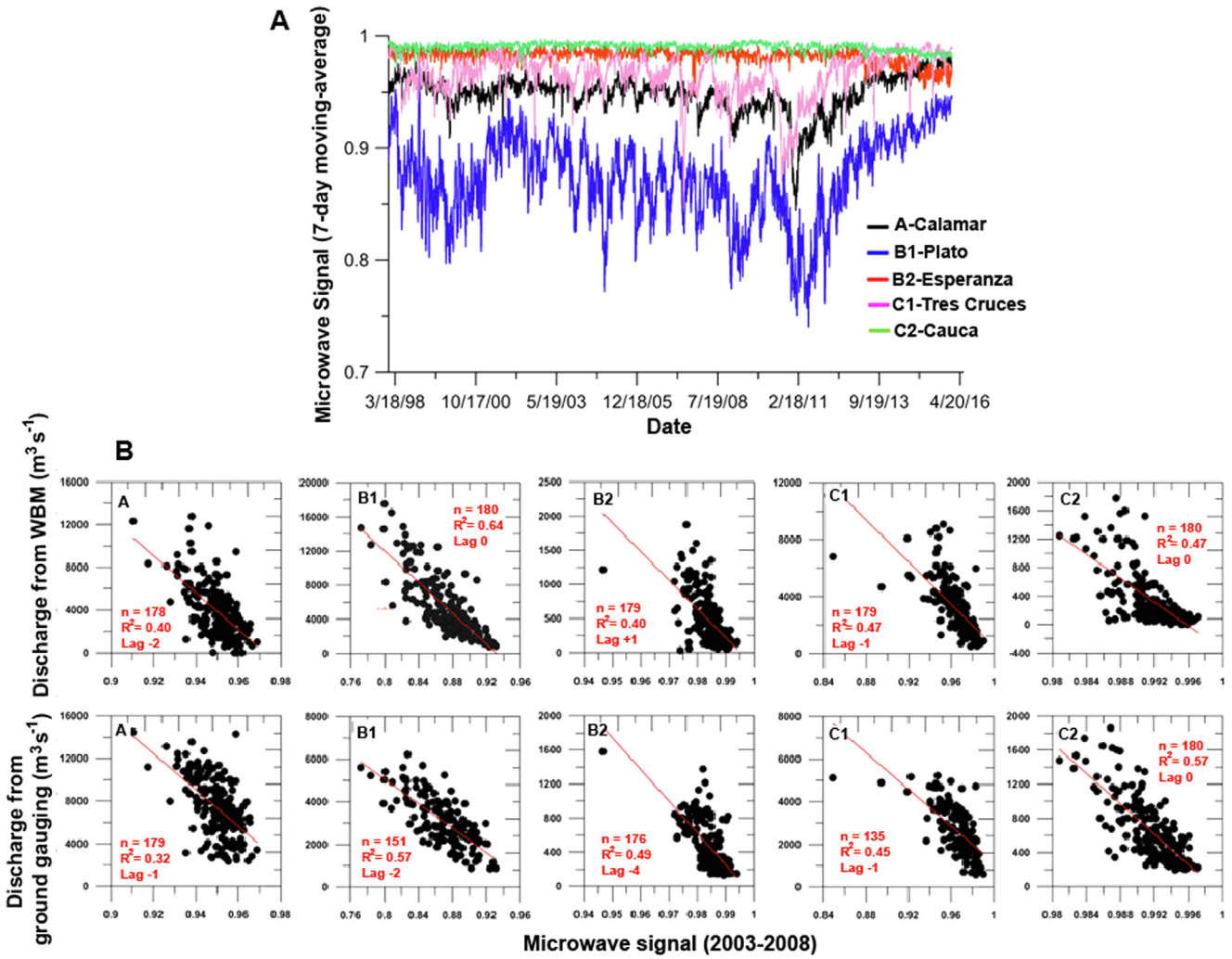

Fig. 7. (A) Timesseries of daily microwave satellite data developed by the Joint Research Center (JRC), Italy, at the satellite stations in the Magdalena River (Fig. 1B). (B) Regression fits between microwave signal and simulated discharges from WBM and ground models at the DFO satellite sites in the Magdalena River.

bands were used to visualize suspended sediment spills into adjacent lakes (Fig. 3).

We constructed timeseries of different connectivity stages by using MODIS images derived black (non-turbid) and white (turbid) freshwaters as tracers in order to establish at what water level and therefore associated satellite derived water discharge each floodplain starts to flood. Four stages of connectivity were identified: (1) river recharge (hydrological connection to floodplain as evidenced by floods), (2) channel-connection between river and floodplain (as evidenced by white, turbid waters), (3) receding flows towards disconnection, and (4) disconnection (Figs. 3 and 6). The gauged water level fluctuation is well replicated by the satellite derived water discharges in both floodplain sites (Barbacoas lagoon and Momposina depression) during neutral and La Niña conditions of 2010–2013, although there are differences in the cumulative coefficient of variation (Fig. 6). For example, freshwater lakes of the Momposina depression show a clear phase-lag between water level and satellite-based water discharges (Fig. 6), indicating that as water level rises, the water still has to pass through a more complex lagoon system before being detected. Thus, the observed phase-lag is possibly related to the hydrological dynamics of channel-floodplain connections. Nevertheless, stages of river-floodplain connection, visualized using daily MODIS satellite images, were superimposed to series of water level and satellite-based water discharge during La Niña, El Niño and neutral years (e.g., Fig. 3D-F and 5). According to the identified thresholds of river-lagoon connectivity (Fig. 6), percentages of connection time were estimated from frequency histograms of water level and satellite-based water discharge series (Fig. 5).

Main statistics of water level (m) and satellite-based water discharge ($m^3\ s^{-1}$) at Barbacoas lagoon and the Momposina depression floodplain, during periods of La Niña, El Niño and neutral years are shown in Table 2. Percentages of time of river-floodplain connectivity obtained by utilizing satellite-based discharges and gauging station water level are very similar, indicating that once connectivity thresholds are defined for each floodplain system, satellite-based timeseries are a good indicator of river floodplain connectivity. In addition, annual flood maps developed by DFO at Barbacoas lagoon and the Momposina depression show that annual flood frequencies (%) observed in channels next to the floodplains (Fig. 9) are in agreement with estimated times of connectivity (%) shown in Table 2. However, differences between flood frequencies (%) (Fig. 9) and time of connectivity (%) (Table 2), observed during La Niña years, may be due to the fact that DFO flood frequency maps do not include the strongest La Niña event on record in 2010–2011 or could be biased by clouds as flood frequency results are derived from MODIS optical bands.

5. Discussion and conclusions

For this study, we analyzed timeseries of satellite-based and ground-based gauging water discharge only for the period 1998–2016 (Figs. 1C

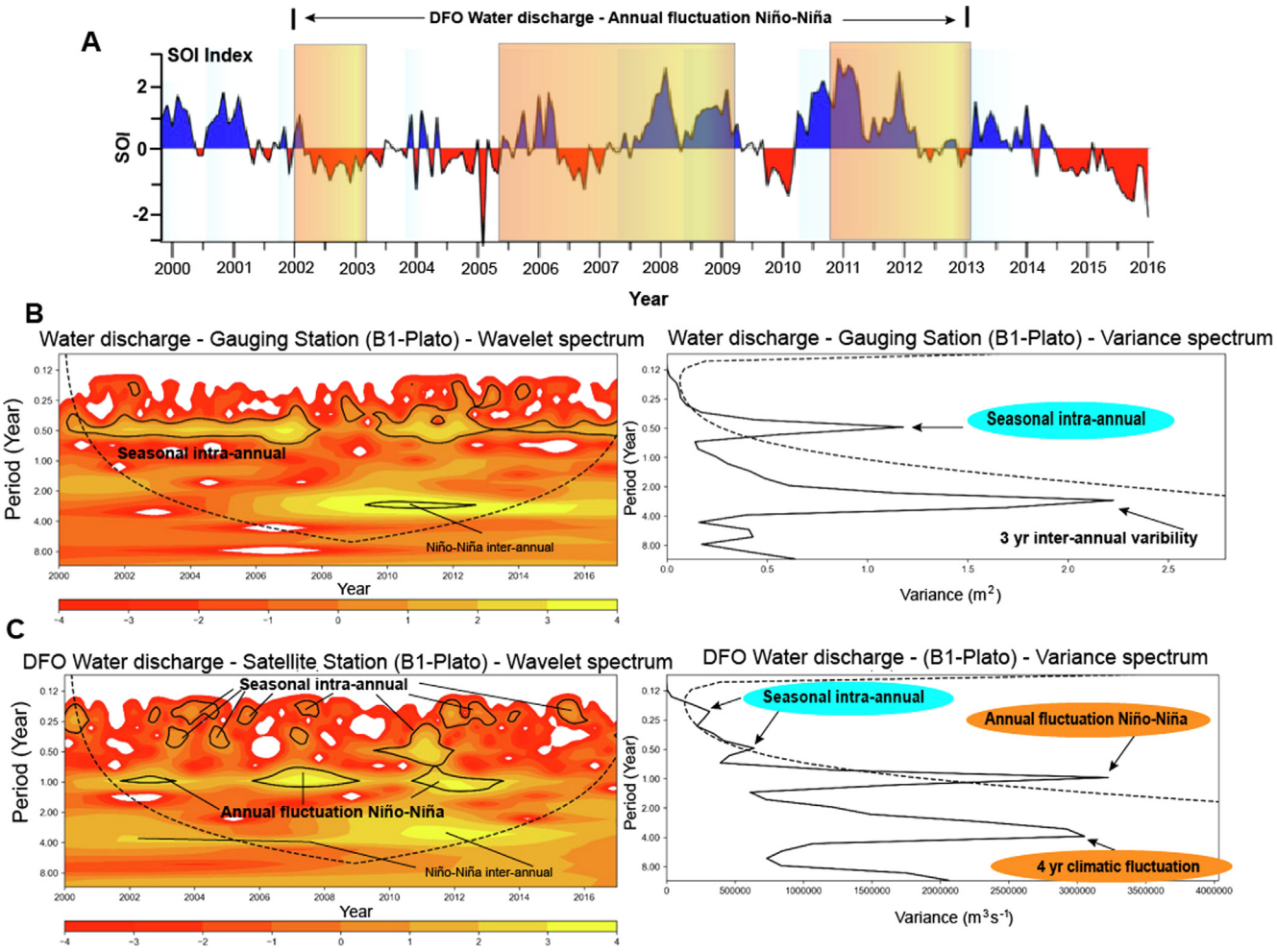

Fig. 8. (A) The Southern Oscillation Index (SOI) showing the period in which the DFO satellite-based water discharge series capture El Niño-La Niña inter-annual variability. (B) Wavelet spectrums of ground-based gauged water discharge and satellite-based water discharge at the Momposina depression floodplain for the period 2000–2016. In the variance spectrums (right B and C) it is shown how well DFO captures the annual seasonality and 4-year inter-annual variability due to El Niño-La Niña cycle compared to ground-based gauged water discharges.

and 8) as more recent ground-based data was not yet released at the time of the study. Nevertheless, satellite-based daily river discharges in near-real-time for the studied sites are updated and made available through the Dartmouth Flood Observatory River Watch portal (http://floodobservatory.colorado.edu/DischargeAccess.html).

River discharge estimated at ground-based gauging stations is well simulated by satellite-based water discharges, especially at the floodplain stations such as Calamar (A), Plato (B1), and Tres Cruces (C1), where the satellite signal properly represents the natural variability of river flow along the Magdalena floodplains (Figs. 1C and 8).

In addition, good correlations between DFO satellite data and ground-based results were observed once lags of one or two months were applied to river discharges with respect to the satellite signal (Table 1 and Fig. 7B). Water discharges at gauging stations are obtained from stage height variations while satellite river flow measurements are based on width variations of the water surface extension.

The existence of consistent lag times between station data and the satellite method requires discussion (Table 1 and Fig. 7B). As noted, ground stations track river discharge changes by river level (stage) at one location. The local relation of actual discharge to stage may change over time with channel bathymetric/morphology changes at the station: stations are in fact often preferentially located to minimize such interference. Also, according to the flow continuity equation ($Q = w*d*v$), stage and flow area both track only particular aspects of discharge: in principle, velocity may be increasing as discharge increases (and a deformable river bed is eroded); stage could remain constant as discharge increases; hysteresis of stage/discharge relations is in fact common (Meade, 1988). Flow area changes for 10 km reaches along large rivers, on the other hand, may exhibit lag times to incoming increasing discharge and also be relatively less affected by local channel erosion or deposition. Thus, while stage normally increases with higher discharge, the water requires time to progressively inundate the local floodplain and change the satellite signal, even if overbank flow is being achieved. Any complex flow dynamics may be integrated, in this way, into the "bulk" water surface area measured each day and as monitored by the sensor: but with some lag time as compared to river stage at one station. This approach thus offers an entirely new way to monitor river flow changes, and advantages and constraints that complement those posed by traditional ground gauging stations.

The analysis of lag times between water level data and satellite observations also requires the consideration of the seasonal hysteresis between floodplain lakes water extent and floodplain water level (Rudorff et al. 2014; Park and Latrubesse, 2017). This hysteresis results in dissonance in the lake local-recharge and disconnection thresholds. In general, the water extent slowly increases during the early stages of rising water level and decreases during early falling water level. In rising levels, water extent starts to increase at certain water level thresholds. This shows that the water extent is not sensitive to the river stage changes when the maximum water extent in floodplain is reached. However, water volume in the floodplain is still increasing during this

Table 2
Main statistics of water level (m) and satellite-based water discharge at Barbacoas lagoon and Momposina depression floodplain during 2000–2017, including periods of La Niña, El Niño and neutral years. Percentages of time of river-floodplain connectivity are indicated as well.

Barbacoas Lagoon					*Momposina Depression Floodplain*			
Gauged Water Level	Period 2000–2017	Niña years	Niño years	Neutral years 2012–2013	Period 2000–2017	Niña years	Niño years	Neutral year 2012–2013
Data points (n)	6283	1690	1521	366	.....	274	367	170
Mean (m)	3,44	3,72	3,16	3,20	.....	12,03	8,04	7,70
Max (m)	5,95	5,49	5,95	4,75	.....	15,10	10,70	10,0
Min (m)	1,06	1,06	1,55	2,13	.....	8,62	6,35	5,21
Mode (m)	3,20	3,80	2,80	3,0	.....	13,5	7,2–10,2	6,2–9,8
Standard dev.	0,68	0,67	0,67	0,49	.....	2,06	1,20	1,54
Coef. variation	0,20	0,17	0,21	0,15	.....	0,17	0,14	0,20
Connectivity threshold (m)	4,20	4,20	4,20	4,20	.....	12,0	12,0	12,0
% Time of connectivity	**17%**	**29%**	**11%**	**5%**	.....	**58%**	**8,6%**	**1,13%**
DFO Water Discharge	Period 2000–2017	Niña years	Niño years	Neutral years 2012–2013	2000–2017	Niña years	Niño years	Neutral year 2012–2013
Data points (n)	6533	1941	1522	366	6518	1941	1522	170
Mean ($m^3\ s^{-1}$)	3276	3588	3161	2773	5172	7483	4183	3431
Max ($m^3\ s^{-1}$)	15,085	10,751	15,085	8115	20,118	20,118	16,908	9500
Min ($m^3\ s^{-1}$)	123	509	577	90	57	92	57	1580
Mode ($m^3\ s^{-1}$)	3000	3000	3000	2500	2000	6000	1000	3500
Standard dev.	1374	1360	1320	1252	3306	3718	2981	1110
Coef. variation	0,42	0,37	0,41	0,45	0,64	0,50	0,71	0,32
Connectivity threshold ($m^3\ s^{-1}$)	5000	5000	5000	5500	10,000	10,000	10,000	9000
% Time of connectivity	**21%**	**32%**	**14%**	**3.8%**	**13%**	**38%**	**5%**	**1,7%**

Note: At Barbacoas lagoon, numbers of data points (n) of ground-based gauged water level are not the same as the satellite-based observations of water discharge due to unavailability of ground-based gauged data during some periods. At the Momposina depression floodplain gauging station, water level data is available since November 2010. Thus, for this site, water level thresholds are defined based on statistics during neutral, El Niño, and La Niña years for the period 2010–2016.

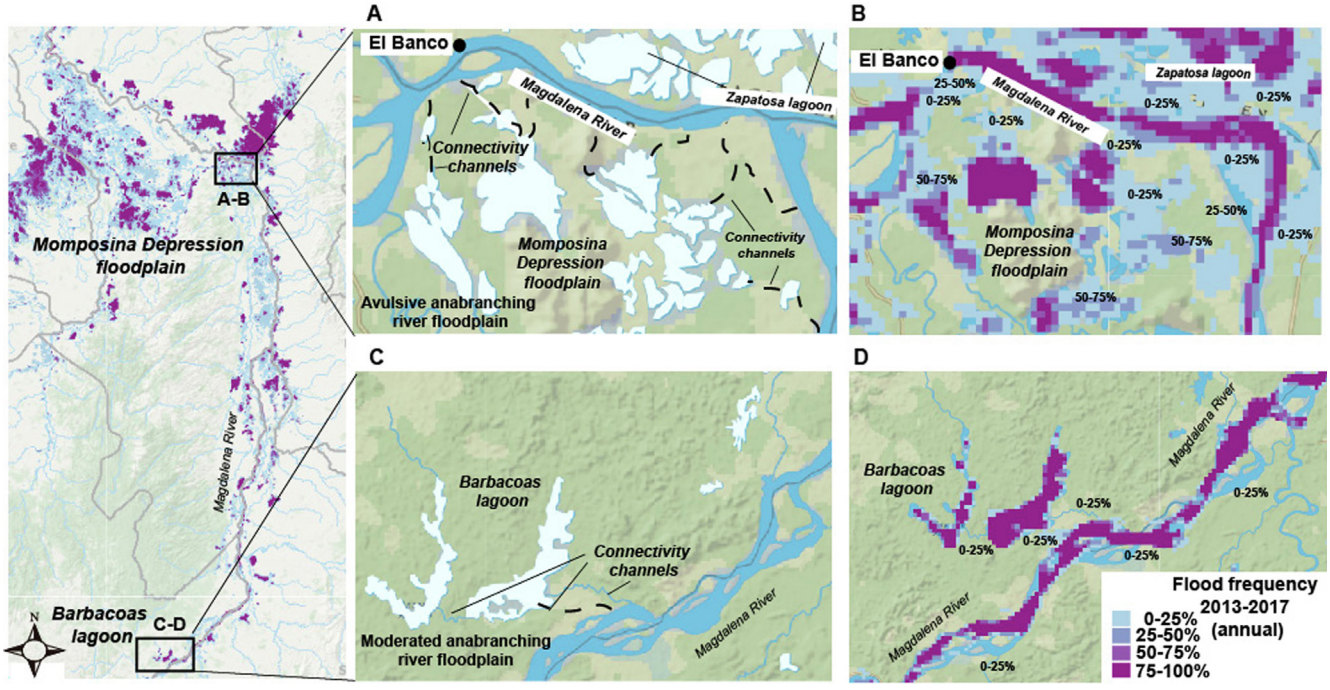

Fig. 9. Remote sensed flood frequency maps at Barbacoas and Momposina depression floodplains (Fig. 1B) during the period 2013–2017, showing percentages of annual flood at each lagoon and their connectivity channels. Observed times of river-floodplain connection by examining frequency distributions of water level and DFO water discharge (Table 2) are of the same magnitude as flood frequencies shown in these maps.

period, as the water from the main channel is continuously being transferred to the floodplain. In general, even before the river bankfull stage (i.e. river stage when it starts to overflow), the floodplain is already saturated and fully covered by water. In the Amazon, for example, water level still increases more than 3 m without changing the water extent (Park and Latrubesse, 2017).

Here, we show the performance of satellite-based discharges to assess preliminary threshold discharges (so stage) of river-floodplain connectivity (Table 2). At downstream stations, discharge variability and magnitudes are well captured by DFO water discharge series (Figs. 1C and 8; Table 1). The applicability of satellite-based discharges is limited at locations on confined channels without floodplains. In

contrast, the changes of water surface area in braided, meandering or anastomosing channels are well correlated to satellite discharge. It is well known that the discharge volume of a given river channel cross-section is exceeded during peak discharge events. In anabranching channels of the Momposina depression floodplain, characterized by lateral connectivity to floodplains (a condition not necessarily related to overbank flows), effective water surface area can maintain a more constant relation to discharge over longer time periods (Smith, 1997; Smith et al., 1995, 1996). Thus, for these conditions, the satellite signal measures more accurately the river discharge magnitude. Our results clearly demonstrate the quality of satellite-based water discharges along stations in the floodplains of the Magdalena River (Fig. 1C, Table 1).

In large anabranching rivers (i.e., Amazon River and the Momposina depression floodplain in the Magdalena River), hydro-geomorphology has to be considered as part of the analysis of hydrological connectivity processes (Drago et al. 2008; Lininger and Latrubesse 2016; Stevaux et al. 2013). In addition to the wide spectrum of the water stage variability, connectivity processes are affected by the complexity of the floodplain hydro-geomorphologic processes, including channelized flow routing paths, overbank diffusion, and local recharge (Latrubesse 2012; Park and Latrubesse, 2017). Therefore, specific studies have to be carried out, in reach by reach, to calibrate individual thresholds of hydrological connection-disconnection levels and flood routing paths that are dependent on the internal geomorphic variability of the floodplain (Park and Latrubesse, 2017). In the Magdalena floodplains further in-situ studies should be conducted in order to understand how the flood pulse is related to the lateral connectivity and the specific river stage thresholds for the hydrologycal connectivity of different geomorphic units.

The capabilities of using satellite data to estimate magnitudes of water discharge during high flow conditions are also shown in this study. During La Niña positive pulses between 2008 and 2011 (Figs. 1C and 8), peak discharges along the Magdalena floodplains were well simulated by the satellite signal, most likely even more precisely than those measured at hydrological gauging stations.

In countries like Colombia, many rivers are not gauged because of the intense civil conflict and the difficulty to access remote and undeveloped river regions. Thus, remote sensing approaches are a useful tool to monitor water discharge and floodplain responses to human induced activities and climate change. According to Sierra et al. (2017), plans to develop monitoring systems that combine satellite data with in-situ measurements are currently being considered by environmental authorities. However, the slow political reaction to establish these monitoring programs does not allow to record current environmental changes in Colombian drainage basins. Scientists can engage policy makers and stake holders such that hydrological monitoring is relevant to decision-making processes, and so environmental policies can be based on the best available scientific data (Salazar et al., 2018). In this study, we show that satellite-derived water discharges are reliable data for river planners and scientists, and also, the support information for exploring hydrological and ecological questions concerning floodplain services, water supply, and flood hazard mitigation.

Declaration of Competing Interest

The authors declare that they have no known competing financial interests or personal relationships that could have appeared to influence the work reported in this paper.

Acknowledgments

This work was supported by the US National Academy of Sciences under the funded PEER project (grant number 70). This paper highlights the collaboration between EAFIT University-Colombia and the DFO – Flood Observatory at the University of Colorado. We also thank the U.S. National Science Foundation, the European Commission's Joint Research Centre (JRC), and NASA through the project Near Real Time Flood Inundation Prediction and Mapping (NNX14AQ44G-NASA). Special thanks to USAID-Colombia for its support on implementing this PEER project in Colombia.

References

Alsdorf, D.E., Rodriguez, E., Lettenmaier, D.P., 2007. Measuring surface water from space. Rev. Geophys. 45, RG2002.
Barletta, M., Jaureguizar, A.J., Baigun, C., Fontoura, N.F., Agostinho, A.A., et al., 2010. Fish and aquatic habitat conservation in South America: a continental overview with emphasis on Neotropical systems. J. Fish Biol. 76, 2118–2176.
Bjerklie, D.M., Dingman, S.L., Vorosmarty, C.J., Bolster, C.H., Congalton, R.G., 2003. Evaluating the potential for measuring river discharge from space. J. Hydrol. 278, 17–38.
Bjerklie, D.M., Moller, D., Smith, L.C., Dingman, S.L., 2005. Estimating discharge in rivers using remotely sensed hydraulic information. J. Hydrol. 309, 191–209.
Brakenridge, G.R., Cohen, S., Kettner, A.J., De Groeve, T., Nghiem, S.V., Syvitski, J.P.M., Fekete, B.M., 2012. Calibration of satellite measurements of river discharge using a global hydrology model. J. Hydrol. 475, 123–136.
Brakenridge, G.R., Nghiem, S.V., Anderson, E., Mic, R., 2007. Orbital microwave measurement of river discharge and ice status. Water Resour. Res. 43, 1–16.
Brakenridge, G.R., Nghiem, S.V., Anderson, E., Chien, S., 2005. Space-based measurement of river runoff. EOS Trans. Am. Geophys. Union 86, 185–192.
Brakenridge, G.R., Knox, J.C., Paylor, E.D., Magilligan, F.J., 1994. Radar remote sensing aids study of the Great Flood of 1993. Eos. Trans. Am. Geophys. Union 75, 521–527.
Bray, W., 2006. Searching for environmental stress: climatic and anthropogenic influences on the landscape of Colombia. In: Stahl, P.W. (Ed.), Archaeology in the Lowland American Tropics: Current Analytical Methods and Applications. Cambridge University Press, New York, pp. 96–113.
Colin, J.G., Smith, L.C., 2014. Toward global mapping of river discharge using satellite images and at-many-stations hydraulic geometry. Proc. Natl. Acad. Sci. U.S.A. 11, 4788–4791.
De Groeve, T., Brakenridge, G.R., Paris, S., 2015. Global Flood Detection System Data Product Specifications. JRC Technical Report. Available at http://www.gdacs.org/flooddetection/Download/Technical_Note_GFDS_Data_Products_v1.pdf.
De Groeve, T., Kugler, Z., Brakenridge, G.R., 2007. Near Real-time Flood Alerting for the Global Disaster Alert and Coordination System. Proc. ISCRAM 33-40.
Drago, E.C., Paira, A.R., Wantzen, K.M., 2008. Channel-floodplain geomorphology and connectivity of the Lower Paraguay hydrosystem. Ecohydrol. Hydrobiol. 8, 31–48.
Etter, A., McAlpine, C., Phinn, S., Pullar, D., Possingham, H., 2006a. Unplanned land clearing of Colombian rainforests: spreading like disease? Landsc. Urban Plan. 77, 240–254.
Etter, A., McAlpine, C., Wilson, K., Phinn, S., Possingham, H., 2006b. Regional patterns of agricultural land and deforestation in Colombia. Agric. Ecosyst. Environ. 114, 369–386.
Etter, A., McAlpine, C., Possingham, H., 2008. Historical patterns and drivers of landscape change in Colombia since 1500: a regionalized spatial approach. Ann. Assoc. Am. Geogr. 98, 2–23.
Gleason, C.J., Smith, L.C., 2014. Toward global mapping of river discharge using satellite images and at-many-stations hydraulic geometry. Proc. Natl. Acad. Sci. U.S.A. 11, 4788–4791.
Hoyos, N., Escobar, J., Restrepo, J.C., Arango, A.M., Ortiz, J.C., 2013. Impact of the 2010–2011 La Niña phenomenon in Colombia, South America: the human toll of an extreme weather event. Appl. Geogr. 39, 16–25.
Jaramillo-Villa, U., Cortes-Duque, J., Flórez, C., 2015. Colombia anfibia. Un país de humedales. Vol. I and Vol. II. (Instituto de Investigación de Recursos Hidrobiológicos Alexander von Humboldt). http://www.humboldt.org.co/es/estado-de-los-recursos-naturales/item/802-colombiaanfibiav1.
Kettner, A.J., Restrepo, J.D., Syvitski, J.P.M., 2010. A Spatial simulation experiment to replicate fluvial sediment fluxes within the Magdalena River Basin, Colombia. J. Geol. 118, 363–379.
Koblinsky, C.J., Clarke, R.T., Brenner, A.C., Frey, H., 1993. Measurement of river level variations with satellite altimetry. Water Resour. Res. 29, 1839–1848.
Kugler, Z., Nghiem, S.V., Brakenridge, G.R., 2019. L-band passive microwave data from SMOS for river gauging observations in tropical climates. Remote Sens. 11, 835.
Lakshmi, V., Fayne, J., Bolten, J., 2018. A comparative study of available water in the major river basins of the world. J. Hydrol. 567, 510–532.
Latrubesse, E.M., 2012. Amazon Lakes. In: Bengtsson, R Herschy, Fairbridge, R. (Eds.), Lakes and Reservoirs. Springer Verlag, pp. 13–26.
Latrubesse, E.M., 2015. Large rivers, megafans and other Quaternary avulsive fluvial systems: a potential who's who in the geological record. Earth-Sci. Rev. 146, 1–30.
Lininger, K.B., Latrubesse, E.M., 2016. Flooding hydrology and peak discharge attenuation along the middle Araguaia River in central Brazil. Catena 143, 90–101.
Meade, R.H., 1988. Movement and storage of sediment in river systems. In: Lerman, A., Meybeck, M. (Eds.), Physical and Chemical Weathering in Geochemical Cycles. Kluwer, pp. 165–179.
Milliman, J.D., Farnsworth, K., 2011. River Discharge to the Coastal Ocean – A Global Synthesis, first ed. Cambridge University Press, Cambridge.
Park, E., Latrubesse, E.M., 2017. The hydro-geomorphologic complexity of 1 the lower Amazon River floodplain and hydrological connectivity assessed by remote sensing

and field control. Remote Sens. Environ. 198, 321–332.
Plazas, C., Falchetti, A.M., Van der Hammen, T., Botero, P.J., 1988. Cambios ambientales y desarrollo cultural en el Bajo Río San Jorge. Bol. Mus. Oro Banco Repúb. 20, 58–59.
Poveda, G., Jaramillo, A., Gil, M., Quiceno, N., Mantilla, R., 2001. Seasonality in ENSO related precipitation, river discharges, soil moisture, and vegetation index (NDVI) in Colombia. Water Resour. Res. 37, 2169–2178.
Poveda, G., Waylen, P.R., Pulwarty, R.S., 2006. Annual and inter-annual variability of the present climate in northern South America and southern Mesoamerica. Palaeogeogr. Palaeoclimatol. Palaeoecol. 234, 3–27.
Restrepo, J.D., Escobar, H.A., 2018. Sediment load trends in the Magdalena River basin (1980–2010): anthropogenic and climate-induced causes. Geomorphology 302, 76–91.
Restrepo, J.D., Escobar, R., Tosic, M., 2018. Fluvial fluxes from the Magdalena River into Cartagena Bay, Caribbean Colombia: trends, future scenarios, and connections with upstream human impacts. Geomorphology 302, 92–105.
Restrepo, J.D., Kettner, A., Syvitski, J.P.M., 2015. Recent deforestation causes rapid increase in river sediment load in the Colombian Andes. Anthropocene 10, 13–28.
Restrepo, J., Ortíz, J.C., Pierini, J., Schrottke, K., Maza, M., Otero, L., Aguirre, J., 2014. Freshwater discharge into the Caribbean Sea from the rivers of Northwestern South America (Colombia): magnitude, variability and recent changes. J. Hydrol. 509, 266–281.
Restrepo, J.D., Kjerfve, B., Restrepo, J.C., Hermelin, M., 2006. Factors controlling sediment yield from a major South American drainage basin: the Magdalena River, Colombia. J. Hydrol. 316, 213–232.
Restrepo, J.D., Syvitski, J.P.M., 2006. Assessing the effect of natural controls and land use Chane on sediment yield in a Major Andean River: the Magdalena drainage Basin, Colombia. Ambio 35, 44–53.
Restrepo, J.D., Kjerfve, B., 2000. Magdalena River: Interannual variability (1975–1995) and revised water discharge and sediment load estimates. J. Hydrol. 235, 137–149.
Rudorff, C.M., Melack, J.M., Bates, P.D., 2014. Flooding dynamics on the lower Amazon floodplain: hydraulic controls on water elevation, inundation extent, and river-floodplain discharge. Water Resour. Res. 50, 619–634.
Salazar, A., et al., 2018. The ecology of peace: preparing Colombia for new political and planetary climates. Front. Ecol. Environ. 16, 1–7.
Sierra, C.A., Mahecha, M., Poveda, G., et al., 2017. Monitoring ecological change during rapid socio-economic and political transitions: Colombian eco- systems in the post-conflict era. Environ. Sci. Policy 76, 40–49.
Smith, D.G., 1986. Anastomosing river deposits, sedimentation rates and basin subsidence, Magdalena River, northwestern Colombia, South America. Sedimentol. Geol. 46, 177–196.
Smith, L.C., 1997. Satellite remote sensing of river inundation area, stage, and discharge: a review. Hydrol. Process. 11, 1427–1439. https://doi.org/10.1002/(sici)1099-1085(199708)11:10<1427::aid-hyp473>3.0.co;2-s.
Smith, L.C., Isacks, B., Bloom, A., 1996. Estimation of discharge from three braided rivers using synthetic aperture radar satellite imagery: potential application to ungauged basins. Water Resour. Res. 32, 2021–2034.
Smith, L.C., Isacks, B., Forster, R.R., Bloom, A., Preuss, I., 1995. Estimation of discharge from braided glacial rivers using ERS1 synthetic aperture radar: first results. Water Resour. Res. 31, 1325–1329.
Stevaux, J.C., Corradini, F.A., Aquino, S., 2013. Connectivity processes and riparian vegetation of the upper Paraná River, Brazil. J. S. Am. Earth Sci. 46, 113–121.
The Nature Conservancy, Fundación Alma, Fundación Humedales and Autoridad Nacional de Pesca, 2016. Estado de las planicies inundables y el recurso pesquero en la macrocuenca Magdalena-Cauca y propuesta para su manejo integrado. (The Nature Conservancy. Bogotá, Colombia. Bogotá, Colombia). Available at https://www.mundotnc.org/nuestro-trabajo/donde-trabajamos/america/colombia/estado-y-propuesta-para-el-manejo-de-las-planicies-inundables-y-el-recurso-p.xml.
Torrence, C., Compo, G., 1998. A practical guide to wavelet analysis. Bull. Am. Meteorol. Soc. 79, 61–78.
Van Dijk, A.I.J.M., Brakenridge, G.R., Kettner, A.J., Beck, H.E., De Groeve, T., Schellekens, J., 2016. River gauging at global scale using optical and passive microwave remote sensing. Water Resour. Res. 52, 6404–6418.
Walschburger, T., Angarita, H., Delgado, J., 2015. Hacia una gestión integral de las planicies inundables en la cuenca del Magdalena-Cauca. In: Rodríguez Becerra, M. (Ed.), ¿Para dónde va el río Magdalena? Riesgos sociales, ambientales y económicos del proyecto de navegabilidad. Foro Nacional Ambiental-FESCOL, Bogotá, pp. 145–168.

Update

Journal of Hydrology

Volume 590, Issue , November 2020, Page

DOI: https://doi.org/10.1016/j.jhydrol.2020.125123

Journal of Hydrology 590 (2020) 125123

Contents lists available at ScienceDirect

Journal of Hydrology

journal homepage: www.elsevier.com/locate/jhydrol

Corrigendum

Monitoring water discharge and floodplain connectivity for the Northern Andes utilizing satellite data: A tool for river planning and science-based decision-making

Juan D. Restrepo A[a,*], Albert J. Kettner[b], G. Robert Brakenridge[b]

[a] Department of Earth Sciences, School of Sciences, Universidad EAFIT, AA 3300 Medellín, Colombia
[b] Dartmouth Flood Observatory, Community Surface Dynamics Modelling System, University of Colorado, Boulder, CO, USA

ARTICLE INFO

Keywords:
Andes
Magdalena River
Remote sensing
River discharge
Floodplain

ABSTRACT

River discharge data and magnitudes of floods are often not readily available for decision makers of many developing nations, including Colombia. And this while flooding for these regions is often devastating, causing many fatalities and insurmountable damage to the most vulnerable communities. During the wet season, in strong La Niña years, infrastructural damages of over $US 7.2 billion have occurred. Mitigation of such natural disasters lacks data-supported scientific approaches for evaluating river response to extreme climate events. Here, we propose a satellite-based technique to measure river discharge at selected sites for the main northern Andean River, the Magdalena. This method has the advantage of back calculating daily river discharges over a period of two decades, and thus making it possible to calculate return intervals of significant flood events. The study shows that satellite based river discharges well capture a) the inter-annual variability of river discharge; b) the natural seasonality of water discharge along the floodplains; and c) peak discharges that were observed during La Niña conditions between 2008 and 2011. The last is likely more accurate compared to ground-based gauging stations, as ground-based stations tend to overflow during large flood events and as such are hampered to accurately monitor peak discharges. Furthermore, we show that these derived discharges can form the base to study river-floodplain connectivity, providing environmental decision makers with a technique that makes it possible to better monitor river and ecosystem processes.

1. Introduction

Northern Andean rivers have become more vulnerable to floods during recent decades (Restrepo and Escobar, 2018; Restrepo et al., 2018). This as the tropical drainage basins, including the large Magdalena River (Fig. 1), have experienced accelerating deforestation and soil erosion rates during the 1980–2010 period (Restrepo and Syvitski, 2006). The Magdalena River, one of the main suppliers of sediment to the ocean (180 Mt y^{-1}) (Restrepo et al., 2015; 2006;; Restrepo and Kjerfve, 2000), has witnessed rising trends in sediment transport during the last three decades. These increasing fluxes correlate well with the observed tendencies in land conversion and deforestation (Restrepo et al., 2015). An important part of the observed increasing sediment flux is being sequestered in riverbeds and along its adjacent floodplains (Kettner et al., 2010; Restrepo and Escobar, 2018), making these Andean rivers less resilient in regulating strong hydrologic pulses during extreme climate events.

In addition to human-induced activities affecting soils, sediment fluxes and the hydrological cycle, the northern Andean basins (Fig. 1B) experience high rainfall rates and associated runoff excess over steep slopes (Restrepo and Syvitski, 2006; Restrepo et al., 2006). Also, the drainage basins are influenced by the El Niño Southern Oscillation (ENSO), which causes dry conditions during the El Niño phase and periods of wet waves during La Niña positive phase. River discharge inter-annual variability is in agreement with the El Niño-La Niña cycle at periods of 3–5 years (Poveda et al., 2001; 2006). Between 2008 and 2011, strong La Niña conditions impacted the northern basins of Colombia and caused economic losses of over $US 7.2 billion (Hoyos et al., 2013).

During La Niña event in 2011, Colombia experienced the strongest floods on record, flooding the country for almost three months by the so called “wet wave” (Hoyos et al., 2013). River authorities and the

DOI of original article: https://doi.org/10.1016/j.jhydrol.2020.124887
* Corresponding author.
E-mail address: jdrestre@eafit.edu.co (J.D. Restrepo A).

https://doi.org/10.1016/j.jhydrol.2020.125123
Received 22 May 2020; Accepted 27 May 2020
Available online 23 June 2020
0022-1694/

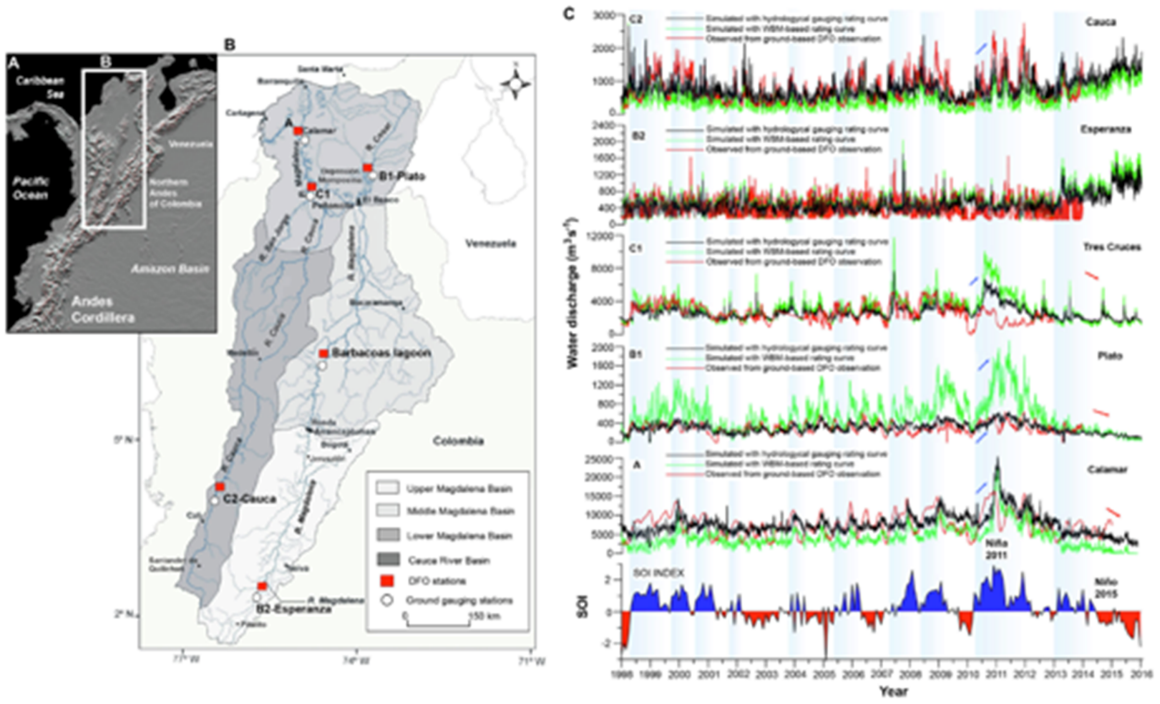

Fig. 1. (A) Northern Andes of Colombia. (B) Ground-based gauging stations and Dartmouth Flood Observatory (DFO) stations used to estimate water discharge and river-floodplain connectivity for the Magdalena River. (C) Water discharge timeseries along the Magdalena River obtained from rating equations utilizing the Water Balance Model (WBM) simulations (green line) and data from hydrological ground gauging stations (black line) (Table 1). The red line shows river flows at each ground-DFO station. We also show the Southern Oscillation Index (SOI) during the 1998–2016 period. period (from Escobar et al., 2017; https://link.springer.com/chapter/10.1007/978-3-319-43744-6_1) (For interpretation of the references to color in this figure legend, the reader is referred to the web version of this article.)

national disaster office however, lack consistent discharge data for drainage basin planning and flood hazard mitigation (Walschburger et al., 2015). In developing countries like Colombia, the flood alert system is based on records of hydrological gauging stations, which are often poorly calibrated and as such lack accuracy if data is made available at all (Restrepo et al., 2006). River fluxes are underestimated when extreme discharges exceed bank-full discharge. In addition, rating curves are not recalibrated after major floods during La Niña events, resulting in unreliable river discharge magnitudes (Milliman and Farnsworth, 2011).

Water observations in many developing countries are constrained by lack of adequate gauge stations. Many agencies that collect the streamflow or precipitation data are not likely to share this data with others. Thus, the lack of in-situ water data from most of the large river basins of the world implies that we can only use the readily available satellite data sets and global land model outputs. The quasi-global coverage provided by satellite observations combined with open data policies can help avoiding the issues related to data access and continuity (Lakshmi et al., 2018).

For the Magdalena, the best gauged Colombian river (Restrepo et al., 2006), most gauging data are updated and made available for users with a two-year time lag. Therefore, environmental authorities, stakeholders, decision makers, and scientific users do not have access to near-real-time information of river discharge, even when extreme events are unfolding. As such, for many river reaches, satellite-derived discharge estimates offer the only reliable data related to fluvial discharges and flood magnitudes. Therefore, implementing satellite-based tools for near-real-time estimation of river runoff provide support to river planning authorities by making data timely available to scientists and decision makers.

Insufficient and less reliable discharge data also makes it more difficult, if not impossible, to establish river-floodplain hydrologic connectivity relationships. The Momposina depression (Fig. 1B), a significant part of the Magdalena floodplain that covers 10% of the catchment area, is the largest avulsive river system in the northern Andes and consists of the least studied fluvial lakes of major South American Rivers (Latrubesse, 2015; Restrepo and Escobar, 2018). Their ecosystem services provide refuge to aquatic biota and has the capacity to act as a buffer to downstream flooding while supplying potable and irrigation water, and they are recognized as nursery areas for fish species used by artisanal fishery (Jaramillo-Villa et al., 2015). However, ongoing human activities along the whole basin have dramatically changed these vital but fragile ecosystems (Barletta et al., 2010).

According to preliminary environmental assessments, more than 30% of the floodplain lakes along the entire Magdalena River have lost their natural fluvial connection, and many of those lakes as such have diminished or disappeared completely during the last two decades (The Nature Conservancy, 2016). Important questions about the connectivity and hydrological functioning of these floodplains still remain unsolved, including: (1) how has the floodplain morphology changed during the last decades in terms of connectivity with the main river and its flooded areas?; (2) what are the hydrological dynamics of floodplains in terms of recharge water level thresholds?; (3) what are the spatial and temporal dynamics of suspended sediment concentration and how does these processes impact the carbon flux through the food webs in the lakes?; (4) how will hydropower development in the basin change river-floodplain connectivity?; (5) how will the Magdalena navigation project impact floodplain connectivity in the many river reaches in which dredging and course changes are proposed? To answer these questions, it is evident that base-line data is needed, including reliable hydrologic time series to be able to analyze river-floodplain connectivity.

During the last two decades, satellite data have provided spatially and temporally dense river discharge mapping from space (e,g., Alsdorf et al., 2007; Bjerklie et al., 2003; 2005a, 2005b, 2007c; Brakenridge

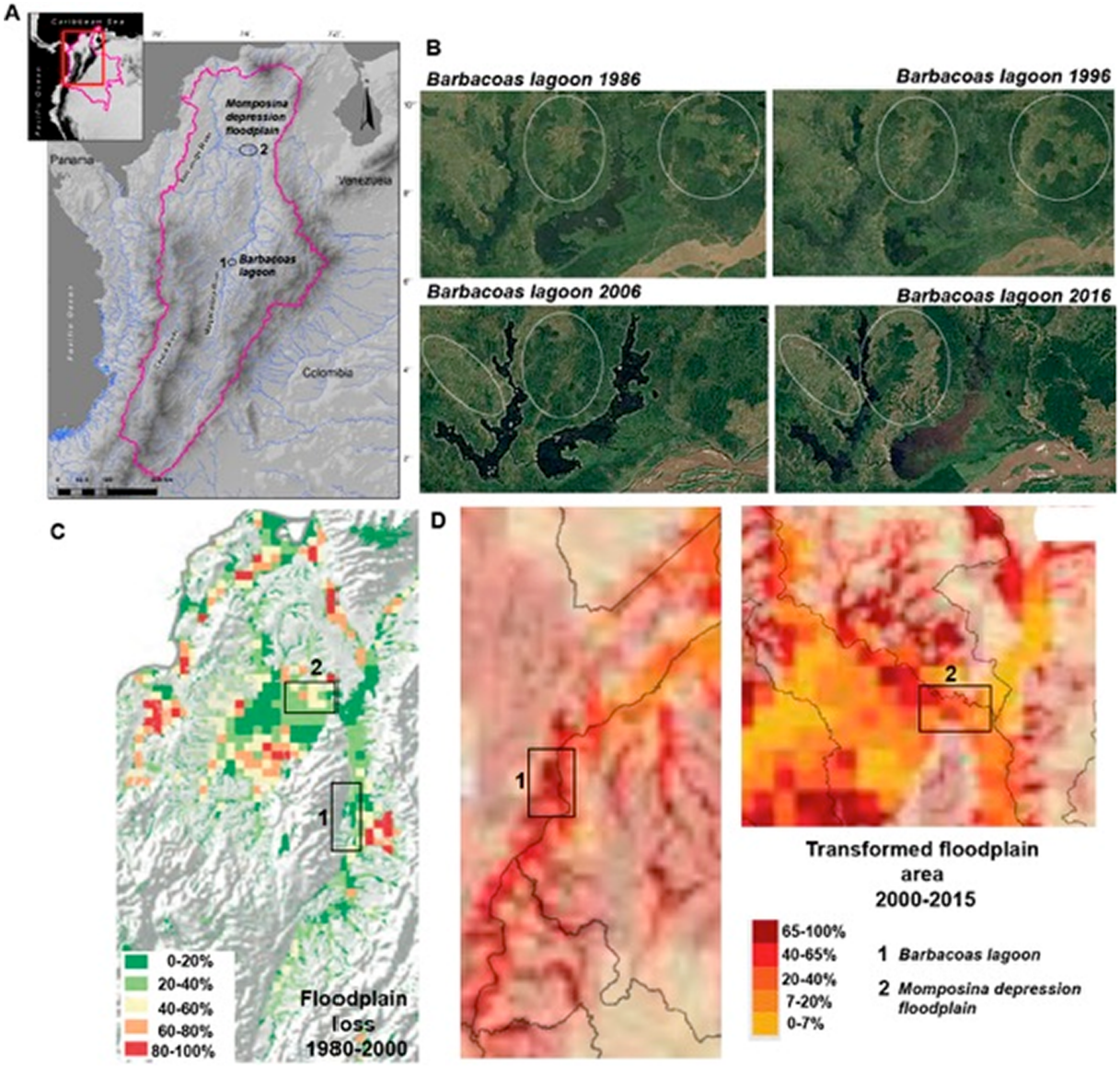

Fig. 2. (A) Magdalena River drainage basin showing the two analyzed floodplain sites, the Barbacoas laggon and the Momposina depression. (B) LandSat images of the Barbacoas lagoon showing areas of deforestation for cattle ranching between 1996 and 2016. (C-D) Assessments of floodplain loss and land transformed area in the Magdalena floodplains (The Nature Conservancy, 2016).

et al., 1994; Colin and Smith, 2014; Gleason and Smith, 2014; Koblinsky et al., 1993; Van Dijk et al., 2016). Although these studies highlight the capabilities of satellite data to monitor river discharge, available tools to monitor river flow in real time were not available until recently. The Dartmouth Flood Observatory (DFO) developed the first tools to estimate near-real-time discharge from world-rivers utilizing the Moderate Resolution Imaging Spectro-radiometer (MODIS) in river reaches (Brakenridge et al., 2005). Also, the Advanced Microwave Scanning Radiometer (AMSR-E) was utilized to obtain river flow by monitoring water surface changes along specific 10 km river reaches. These satellite data applications showed that microwave sensors are accurate for monitoring rive with a daily frequency of 1–2 days with the advantage of having low interference from clouds (Brakenridge et al., 2007). Additional work has since explored further general applicability of the approach (Kugler et al., 2019; Van Dijk et al., 2016).

Over the years, DFO has optimized the process of deriving river discharge from satellite data, and can now estimate discharges even for ungagged rivers (Brakenridge et al., 2012; De Groeve et al., 2007), by utilizing a global hydrological model, the global Water Balance Model (WBM) for calibration (Brakenridge et al., 2012). Currently, the Dartmouth Flood Observatory (http://floodobservatory.colorado.edu), River watch version 3.5 measures river discharge in hundreds of reaches along many rivers around the world. To ensure long timeseries of quasi daily data, River Watch stations are based on the passive microwave signals from AMSR-E, AMSR2, TRMM and GPM, processed in collaboration with the Joint Research Centre (JRC) (Brakenridge et al., 2012), allowing to retrieve data from January 1998 onwards (De Groeve et al., 2007).

Northern Andean rivers have become more vulnerable to floods during the last decades. This as land-use changes and deforestation have made these rivers less resilient in buffering strong hydrologic pulses during extreme climatic events. River authorities and flood mitigation planning lack however, adequate science-supported tools for evaluating river response to extreme climate and human induced events. Here, we use the satellite derived microwave radiometry signal as a tool for estimating near-real-time water discharge for the main northern Andean River, the Magdalena. Stream-flow timeseries during 1998–2016 were obtained and analyzed for six sites along the

Table 1
Mean water discharge values and rating equations obtained from the WBM-based model, ground-based DFO model, and five gauging stations of the Magdalena River. Accuracy statistics, including the DFO R^2 quality levels and signal-noise rating (S/N) are shown (De Groeve et al., 2015). Best regression determination coefficients (r^2) between the satellite signal and WBM and ground-based DFO model simulations are shown after applying 0 and −2 months lags (gray). The *p*-values of the regression between WBM and the ground-based DFO model are also shown.

Site ID	Lat-Long	Channel pattern	Mean discharge WBM-based model ($m^3 s^{-1}$)[a]	Mean discharge Ground based DFO model ($m^3 s^{-1}$)[b]	Mean discharge gauging station ($m^3 s^{-1}$)[c]	Gauging station-based equation[d]	R^2	R^2 quality	S/N rating	Accuracy	Lag (months)	r^2 WBM-based model	*p* Value	r^2 Ground-based DFO model
A	10.214 -74.924	Moderated anabranching	4420.82	7650.67	7667.71	y = -170,746.49x + 169,553.97	0.32	1	1	1	-2	0.40	0.016	0.22
B1	8.954 -73.934	Avulsive anabranching	5518.63	2963.19	3120.00	y = -28,722.65x + 28,047.70	0.57	2	1.5	1.75	0	0.64	0.0001	0.32
B2	2.744 -75.374	Meandering	549.16	505.87	395.27	y = -34,041.30x + 33,968.17	0.49	2	1	1.5	0	0.37	0.068	0.43
C1	8.594 -74.564	Anabranching	3051.16	2633.93	2642.99	y = -42,939.55x + 44,086.00	0.45	2	2	2	-1	0.47	0.015	0.45
C2	3.824 -76.364	Meandering	485.68	794.04	748.72	y = -89,021.55x + 88,924.22	0.57	2	1	1.5	0	0.48	0.072	0.57

Note: a) River discharge estimates from the Water Balance Model (WBM); b) Water discharge estimates from the ground-based DFO-River Watch microwave signal; c) Water discharge from hydrological gauging stations obtained from from Instituto de Hidrología, Meteorología y Estudios Ambientales, IDEAM; d) Transformation of the remote sensing signal to river discharge values is performed using a rating equation. The calibrated discharge values were obtained via rating equations produced in two different ways: 1) via discharge values derived from WBM and 2) via hydrological gauging stations.

Magdalena channel for independent and efficient evaluation of discharge variability, flood magnitude estimations and river-floodplain connectivity thresholds. In this study we show that for large, less well-gauged river basins, satellite-based observations are useful for river planners and flood hazard mitigation efforts.

2. Study area

Drainage basins in Colombia are unique Andean fluvial systems due to their geographical setting. Near the Ecuadorian border, the Andes mountain range divides in three parallel branches, the Western, Central, and Eastern Cordilleras (Fig. 1A). Between these Cordilleras lie the Magdalena River, the main fluvial system in the northern Andes and the main contributor of fluvial fluxes into the Caribbean (Fig. 1B) (Restrepo and Kjerfve, 2000). The drainage basin covers 25% of Colombia (258,437 km^2) and hosts nearly 80% of the country's population. The river basin consists of tributary systems with high vertical aggradation, an anastomosing river pattern, and subsiding foreland regions (Latrubesse, 2015). The basin experiences natural erosion processes due to high precipitation rates (annual mean of 2,500 mm), steep slopes exceeding 35°, and strong runoff pulses associated to La Niña events (Restrepo and Syvitski, 2006). All these geomorphic conditions favor high rates of sediment supply and transport from the Andes Cordilleras, making the Magdalena River one of the top ranking world rivers in terms of sediment flux (Restrepo et al., 2015; 2006;; Restrepo and Syvitski, 2006).

In addition to natural conditions favoring high rates of sediment yield (Restrepo et al., 2006), human induced impacts such as forest clearance for cattle ranching, agriculture, urbanization and mining, have increased sediment yield rates during the last decades (e.g., Restrepo and Syvitski, 2006; Restrepo et al., 2015). In the Magdalena basin, 80% of the primary forests was cleared by 2000 (Etter et al., 2008) and lowland dry forests were eradicated by 90% (Etter et al., 2006a,b). Therefore not surprisingly, studies of land conversion and sediment transport trends have shown that the magnitude of erosion in the northern Andes has dramatically increased from 500 t km^{-2} y^{-1} to 700 t km^{-2} y^{-1} during the 2000–2010 period, an increase of ~30% (Restrepo et al., 2015).

Human induced changes observed upstream the northern Andean rivers have been also seen downstream along the floodplains (Fig. 2). The floodplains of the Magdalena River, covering 10% of the catchment area, are the largest fluvial fans in the northern Andes and the less well studied fluvial lakes of the major South American Rivers. The floodplains and lakes have important ecosystems services, including: ~50% of the freshwater fishery landings, refuge of aquatic biota, flood control, potable and irrigation water supply, and they are recognized as nursery areas for fish species used by artisan fishery (Jaramillo-Villa et al., 2015). However, the ongoing human activities along the whole basin have dramatically changed these vital ecosystems and fishery landings (Barletta et al., 2010; The Nature Conservancy, 2016). According to some preliminary environmental assessments, more than 30% of the floodplain lakes have lost their natural connections to the main Magdalena River, and many lake systems have diminished considerable or are vanished completely during the last two decades (The Nature Conservancy, 2016) (Fig. 2).

There is no doubt that increasing trends in, and pulses of, upstream sediment transport have made Colombian rivers less resilient to regulate strong hydrologic pulses during extreme climate events. A significant part of the observed increasing fluxes of sediments is becoming sequestered in lakes and or reservoirs, river channels and along the adjacent floodplains (Kettner et al., 2010; Restrepo and Escobar, 2018). Once the Magdalena River crosses the more flood prune area of the Momposina depression (Fig. 1B and 3), overflow and levee failures will become more common, causing extensive flooding from April until November. At the Momposina depression alone, sedimentation of 3–4 mm y^{-1} over the last 7,500 yr has formed a 130-m-thick deposit (Bray, 2006; Plazas et al., 1988; Smith, 1986). Based on a sediment transport conceptual model, Restrepo et al. (2006) found that 16% of the total annual sediment flux is deposited in the Momposina floodplains alone. Further analysis based on LandSat and MODIS images (Kettner et al., 2010), calculations of sediment load (Restrepo and Escobar, 2018), and sedimentation rates at the downstream Magdalena reaches (Plazas et al., 1988), indicate that approximately 20–80 Mt y^{-1} of sediment is deposited in the Momposina depression floodplains.

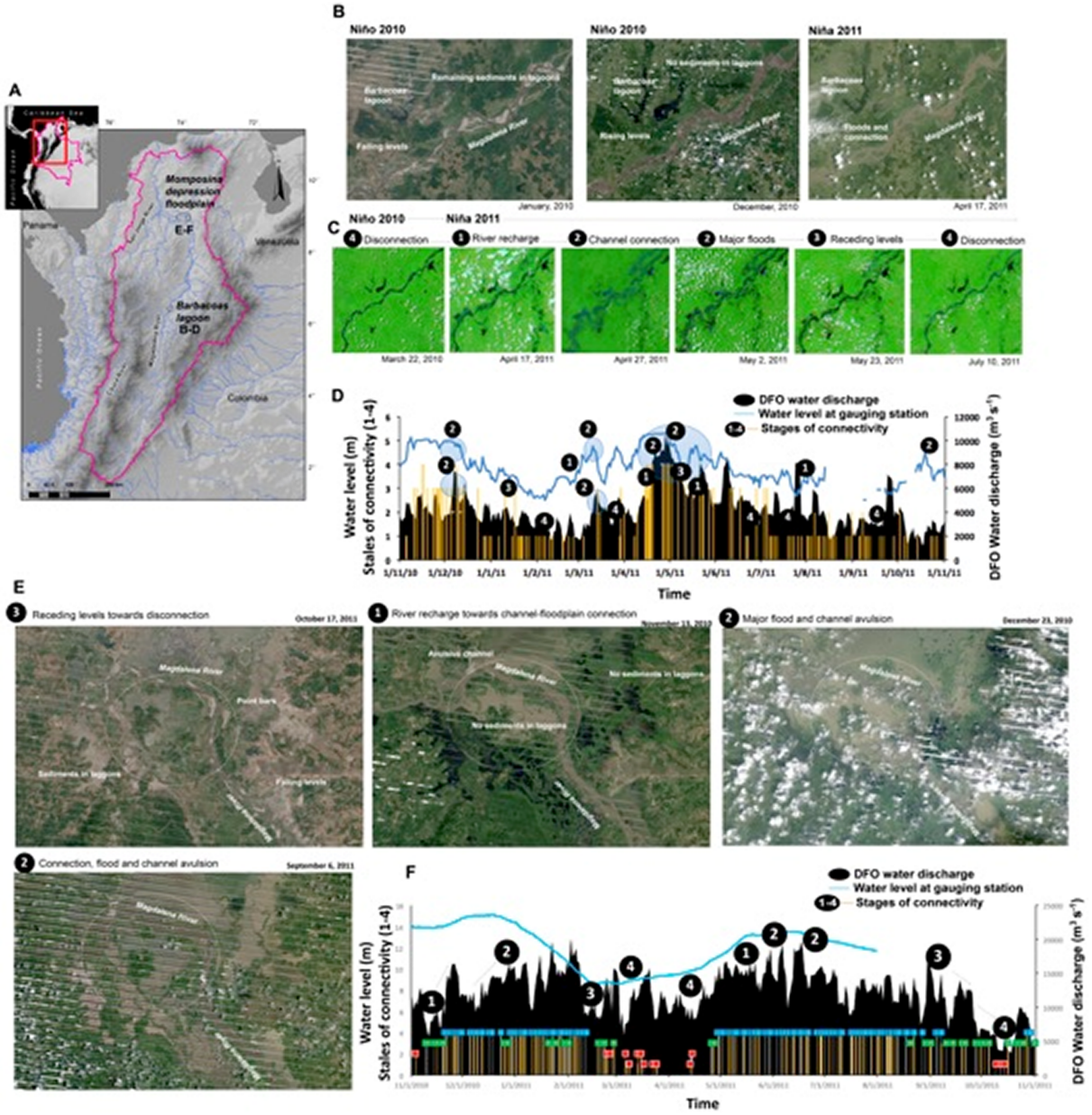

Fig. 3. (A) Magdalena River drainage basin showing the two analyzed floodplain sites, the Barbacoas laggon and the Momposina depression. LandSat (B) and MODIS satellite images (C) showing stages of river-floodplain connectivity for the Barbacoas floodplain during El Niño-La Niña cycle 2010–2011. (D) Time series of satellite-based water discharge, gauged water level, and states of river-floodplain connectivity observed in the Barbacoas lagoon by analyzing daily aqua and terra MODIS satellite images. (E) LandSat satellite images for the Momposina depression showing stages of river-floodplain connectivity. (F) Stages of river-floodplain connectivity for the Momposina depression during 2010–2011.

All these mentioned environmental facts, including upstream land conversion, deforestation, increasing trends in erosion, and large amounts of sediment trapping downstream, strongly indicate that the Magdalena floodplains are becoming less resilient to floods due to human induced impacts and increasing pulses of sediment flux.

3. Methods

Satellite microwave sensors like TRMM, AMSR-E, AMSR-2, and GPM have a global coverage with a daily return period, and for certain wavelengths the earth surface can be monitored despite cloud cover. Brakenridge et al. (2005) and Van Dijk et al. (2016) showed that by utilizing these sensors, river discharge can be monitored. Applying similar techniques of how discharge is measured on the ground, namely by measuring stage height, variation in the microwave signal reflect changes of river width. So, as water discharge increases, the width of a river increases and therefore the microwave signal changes (Brakenridge et al., 2007; 2012). The microwave data has typically a spatial resolution of 10x10km, which is sufficient, when located over a river, to observe discharge variation over time as long as the area includes both land (high emission) and water surfaces (low emission). The data is inverse in that as water rises (so the area of the water increases) the total emitted radiation reduces as land surface area becomes smaller for that pixel. With the use of the hydrologic model WBM (the Water Balance Model) this microwave signal can be translated into a discharge. Recently, Lakshmi et al. (2018) have demonstrated the application of the satellite-based WBM on estimating available water in the major global river basins. The authors show how the WBM can be used to estimate total water fluctuations and to compare hydrologic spatial and temporal variations across large hydrologic regions. This

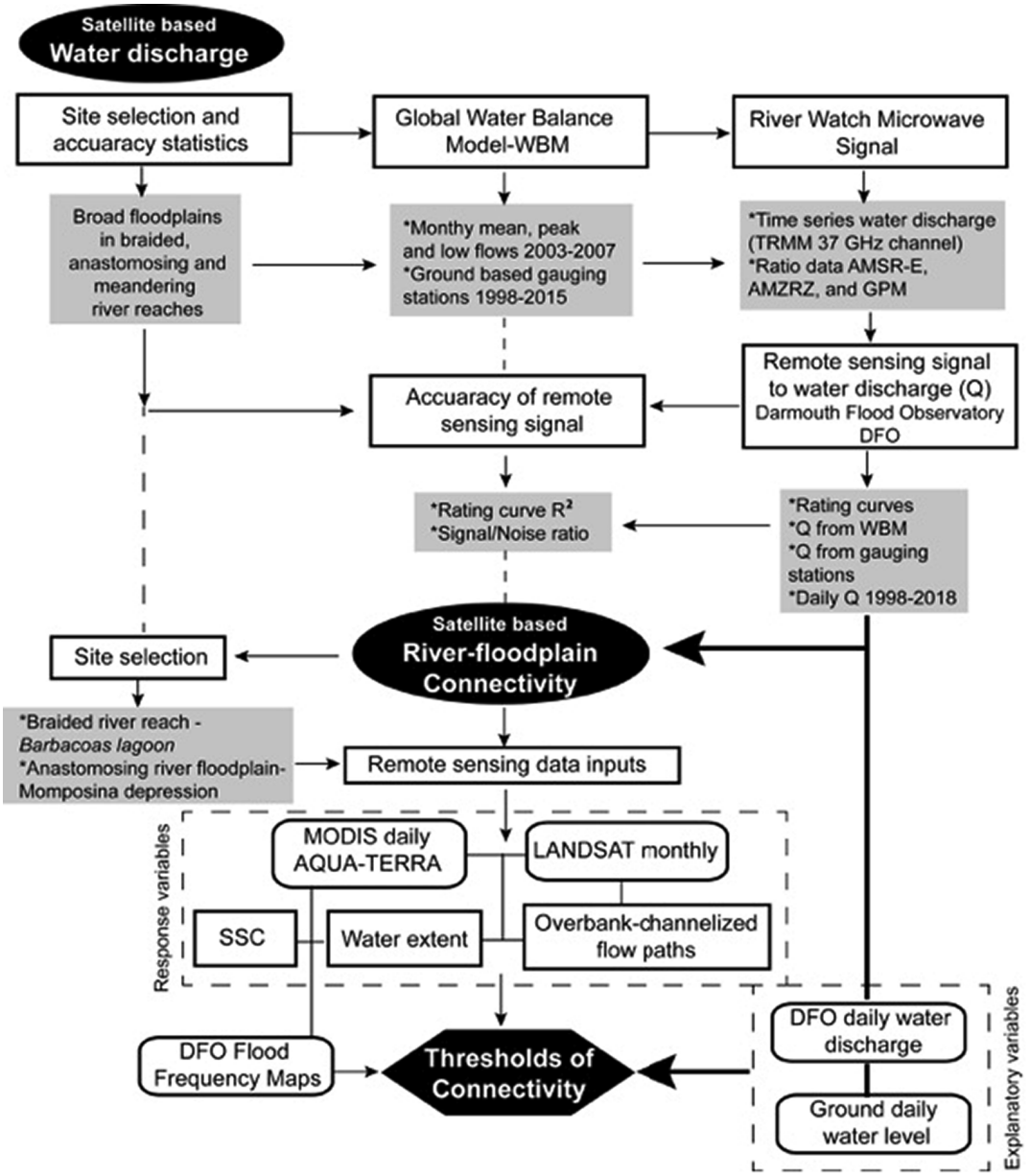

Fig. 4. Scheme of main analyses conducted to estimate water discharge and river-floodplain connectivity using satellite-derived data produced by DFO.

technique has been applied for many rivers at the Dartmouth Flood Observatory and is made semi-operational through the River Watch 3.5 system (Brakenridge et al., 2012).

For the Magdalena River, six sites (Fig. 1B) were selected for which both satellite-based observations as well as ground based gauged data were obtained. The ground-based gauge data was obtained from the Hydrological and Environmental Institute of Colombia, IDEAM. A simple regression function is normally established between the hydrological modeled data and the satellite microwave data. For this study also a regression function was established by using the ground based gauged data. This to assess the model-based and ground gauged-based rating curves for model bias and accuracy of the Riverwatch System (Brakenridge et al., 2012) (Table 1). Accuracy of rating curves and data from selected hydrological gauging stations were assessed in previous studies along the Magdalena River (e.g., Restrepo et al., 2006, 2015; Kettner et al., 2010).

So, to obtain timeseries of satellite-derived water discharge during the 1998–2016 period (Fig. 1C), we used both modeled discharge as observed discharges and: (1) established a rating curve between gauged data and the microwave data to generate daily discharges for the period of interest (Table 1), (2) established a rating curve between modeled data and the microwave data to generate daily discharges for the period of interest, (3) applied accuracy assessments and stats on how discharges are performing based on the satellite signal as compared to gauging sites (Table 1), and (4) improved the fitness of the rating curves through calibration equations between gauging station discharge and modeled WBM discharge, after applying different lag times.

To assess the application of satellite-derived water discharge series to identify thresholds of river-floodplain connectivity, we selected two different floodplain sites: the Barbacoas lagoon, a confined floodplain in a meandering river reach, and the Momposina depression system, an avulsive anabranching floodplain (Fig. 1B and 3). Daily near-infrared aqua and true-color terra moderate resolution MODIS satellite images were acquired for the period 2000–2017. Daily images were examined during dry, transition, and wet seasons, as well as during the monsoon (La Niña) and El Niño years. Pixels that over time turn black in the near-infrared MODIS images indicate the extension of floodplain lakes surrounding the Magdalena River and the Momposina region while MODIS

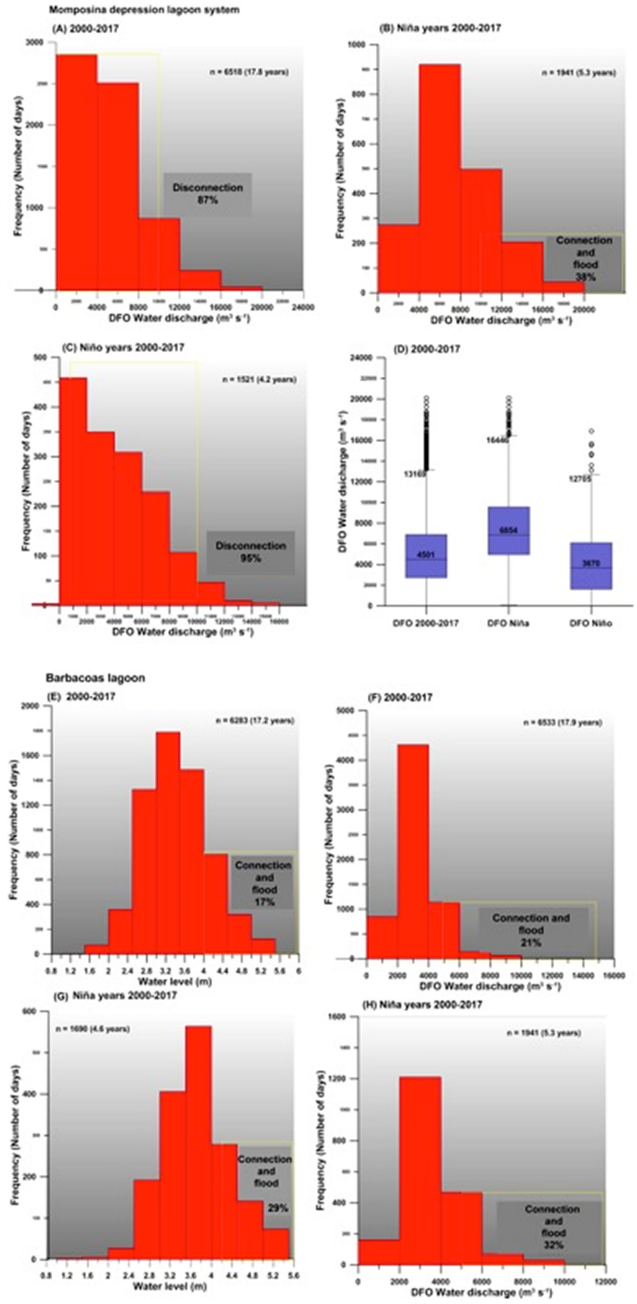

Fig. 5. (A-C) Histograms of estimated satellite-based thresholds of connectivity for the Momposina depression floodplain during the period 2000–2017, including La Niña and El Niño years. The box-whisker plot of satellite-based water discharge during 2000–2007 is also shown (D). (E-H) Histograms of gauged water level and DFO satellite-based thresholds of connectivity for the Barbacoas lagoon during 2000–2017, including La Niña years.

true-color terra images were used to visualize sediment spills of the Magdalena River flowing on the floodplains.

In order to establish at what water level and satellite-based water discharge each floodplain starts to flood, we constructed timeseries of different connectivity stages by using MODIS images derived black (low turbidity) and white waters (higher turbid river waters) as indicator. Four stages of connectivity were identified: (1) river recharge (hydrological connection to floodplain as evidenced by floods), (2) channel-connection between river and floodplain (as evidenced by white waters), (3) receding flows towards disconnection, and (4) disconnection (Figs. 3, 5 and 6). According to the identified thresholds of river- lagoon connectivity (Fig. 6), percentages of connection time were calculated from frequency histograms of water level and DFO water discharge series (Fig. 5).

The main methodological steps followed in this study to estimate water discharge and river floodplain connectivity utilizing the microwave data (De Groeve et al., 2015) are shown in Fig. 4.

4. Results

4.1. Satellite timeseries of river discharge

Six stations along the Magdalena and Cauca Rivers were selected for installation of new River Watch measurement sites (or "satellite gauging sites") (Fig. 1B). Each site is a single 10 km square pixel within a global gridded product developed by the JRC for its "Global Flood Detection System" (GFDS, De Groeve et al., 2015). The morphologies of these river reaches include braided, anastomosing or meandering plane forms and all have distinctive floodplains. Such floodplain units support considerable variations in water surface extension with changes in river flow. The River Watch/GFDS flow area-sensitive signal varies between 0.84 and 0.99 at Calamar (A), while at Plato (B1) the signal varies between 0.72 and 0.96. Other stations, including Tres Cruces, Cauca, and Esperanza, experienced variations between 0.84 and 0.98 (Fig. 7A). This signal is the ratio between emissivity of a pixel that represents the day's driest (the 95th percentile) emissivity within a 9 × 9 pixel array surrounding the emissivity of a selected river - floodplain site. This ratio is used instead of simply the measurement pixel radiance alone in order to remove temporal variation (such as from land temperature) affecting all of the terrain, and isolate the hydrological signal. At the microwave frequency used, increasing in-pixel coverage by surface water as compared to land produces a robust decline in measured radiance, and is much stronger than that observed also by soil moisture changes (Brakenridge et al., 2007).

As expected, sites located in the Momposina depression floodplain, such as Calamar (A), Tres Cruces (C1), and Plato (B1), showed large variability in the signal ratio during the 1998–2016 period (Fig. 7A), a condition that indicates high variability in water surface area. In fact, the station at Plato (B1) displays the more accurate microwave signal after WBM calibration. In contrast, upstream stations with limited floodplains, including Esperanza (B2) and Cauca (C2) (Fig. 1B and 7A), showed weaker satellite detection of water surface variability as clearly seen in the smaller variations of the microwave ratio value (Fig. 7A). However, it was later observed that regardless the small variation in the microwave signal, the values of river discharge at these stations were accurate.

We used WBM simulations and data from five hydrological gauging stations to obtain river discharges (Table 1). Linear regressions and determination coefficients (r^2) between ground and simulated river discharges were calculated for different time lags (months) (Fig. 7B). Regression fits improved once discharge was lagged by some months. For example, at Calamar, determination coefficient r^2 between satellite data and WBM-river discharge ranged from 0.10 at lag 0 months to 0.40 at a lag of −2 months, indicating that the simulated river flow of the WBM model at this site is too fast. WBM is a global model so such routing speed errors for individual rivers are not surprising. However, results in the Momposina depression floodplain at Plato (B1), show that the satellite signal and WBM river discharge are well correlated with a coefficient r^2 of 0.64 with no lag months (Table 1 and Fig. 7B). In addition, satellite data and river discharge from ground-gauging stations are well correlated with $r^2 = 0.57$ at a lag of −2 months (Fig. 7B). Additional regression fits were performed at stations Tres Cruces (C1), Cauca (C2), and Esperanza (B2) with r^2 coefficients between 0.40 and 0.64 (Table 1 and Fig. 7B).

The rating equations obtained from the WBM-based model, ground-based model, and gauging stations at the analyzed sites (Fig. 1B) were used to convert the satellite signal to water discharge (Table 1). Overall, the inter-annual variability observed at ground gauging stations is

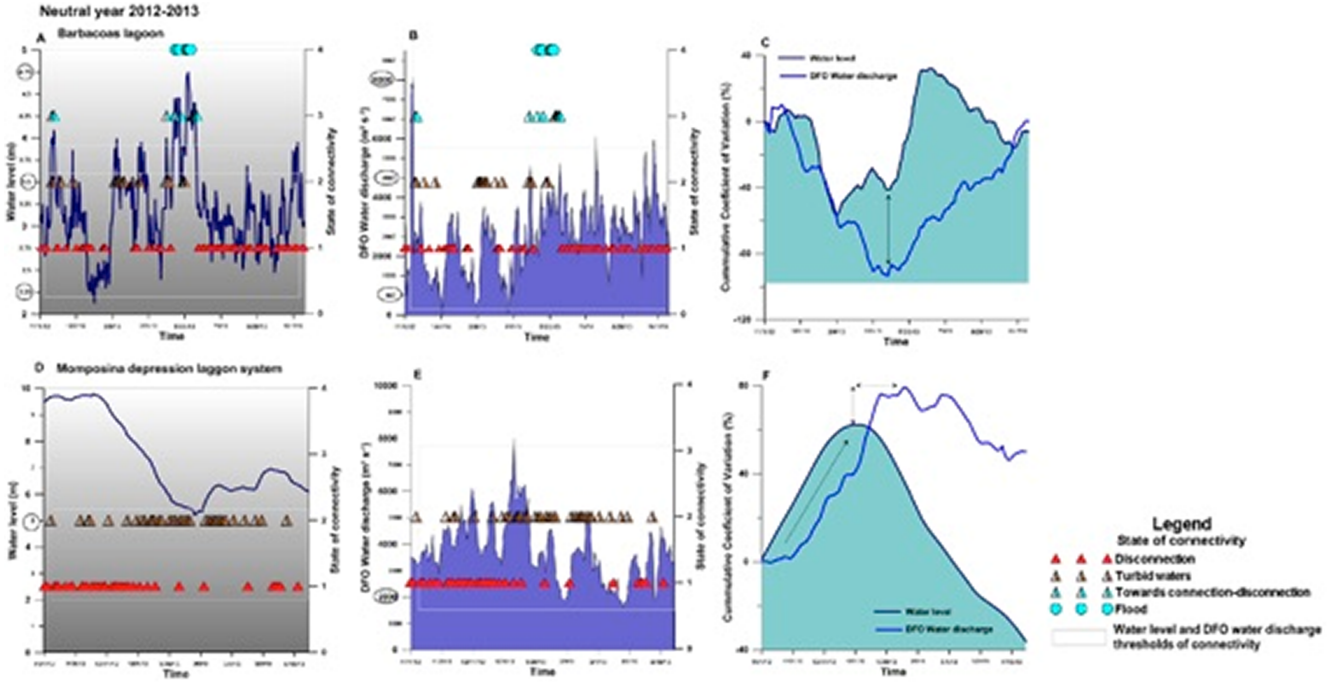

Fig. 6. Examples of timeseries of water level (A, D), satellite derived water discharge (B, E) and coefficient of variation between for water level and satellite derived water discharge (C, F) for the Barbacoas lagoon and the Momposina floodplain during a neutral year 2012–2013. Observed stages of connectivity through MODIS images are superimposed to series in order to define thresholds of connectivity.

followed quite well by satellite-observed river discharges (Fig. 1C). For the stations at Esperanza (B2) and Cauca (C2), the satellite signal captures well the short wave fluctuations, whereas larger variations are observed in the floodplains more downstream at Plato (B1) and Tres Cruces (C1) (Fig. 1C). Here, satellite-observed river discharge follows well the observed discharges at ground gauging stations, especially during high flow conditions. It is worth noting that during peak discharge events, the WBM rating curve overestimates the river discharge magnitudes at Plato (B1) station (Fig. 1C). In general, simulated versus observed river discharges match quite well in the downstream-floodplain stations (Fig. 1C and 7B).

In the upper basin, the satellite site at Esperanza (B2) is located in a narrow channel with limited alluvial plains, downstream two major dams. Here, the satellite signal catches well the short-term fluctuations of observed ground discharges (Fig. 1C). Also, the upstream station at the Cauca tributary (C2) witnessed a good agreement between the satellite river discharges and the observed stream flows (Fig. 1C) despite its location on a constrained river reach with narrow floodplains.

The ENSO cycle is also well captured by the satellite-observed discharge variability (Fig. 1C). During La Niña phase 2010–2011, the magnitudes of measured discharge match well with the Southern Oscillation Index values, whereas low discharge values are observed during El Niño conditions of 2015–2016 (Fig. 1C). However, the upstream Magdalena station at Esperanza (B2) does not exhibit a clear control by the ENSO variability because its river discharge is mainly controlled by the operation of dams.

To evaluate how well time series of satellite-based water discharge capture the observed and measured inter-annual variability related to the ENSO cycle, we used the Continuous Wavelet Transform (CWT) (Fig. 8) (Restrepo et al., 2014; Torrence and Compo, 1998). The CWT function was applied on monthly gauged water discharge and satellite-based discharge at Plato (B1) and used to visualize the periodicities and variability patterns. Clearly, the satellite-based measured discharge properly follows the annual fluctuation as well as the inter-annual variability due to the ENSO oscillation at Plato (B1). The variance spectrum shows that the satellite measured discharge catches significantly better the annual fluctuation and the 2 to 4 years inter-annual variability compared to ground-based gauged river discharge (Fig. 8C, right).

4.2. River-floodplain connectivity thresholds utilizing DFO satellite data

To assess the applicability of satellite derived discharge data on identifying thresholds of river-floodplain connectivity, we selected two different floodplain sites: the Barbacoas lagoon, a confined floodplain system in a meandering river reach, and the Momposina depression, an avulsive, anabranching floodplain (Fig. 1B). Daily near-infrared aqua and true-color terra moderate resolution MODIS satellite images were collected for those areas and analyzed for the period between 2000 and 2016. Satellite based discharge data were downloaded from the DFO River Watch system. Daily images were examined during dry, transition, and wet seasons, as well as during La Niña and El Niño years since 2000. Pixels that over time turn black in the near-infrared MODIS images indicate the extension of floodplain lakes bordering the Magdalena River and the Momposina region, while MODIS terra optical bands were used to visualize suspended sediment spills into adjacent lakes (Fig. 3).

We constructed timeseries of different connectivity stages by using MODIS images derived black (non-turbid) and white (turbid) freshwaters as tracers in order to establish at what water level and therefore associated satellite derived water discharge each floodplain starts to flood. Four stages of connectivity were identified:: (1) river recharge (hydrological connection to floodplain as evidenced by floods), (2) channel-connection between river and floodplain (as evidenced by white, turbid waters), (3) receding flows towards disconnection, and (4) disconnection (Figs. 3 and 6). The gauged water level fluctuation is well replicated by the satellite derived water discharges in both floodplain sites (Barbacoas lagoon and Momposina depression) during neutral and La Niña conditions of 2010–2013, although there are differences in the cumulative coefficient of variation (Fig. 6). For example, freshwater lakes of the Momposina depression show a clear phase-lag between water level and satellite-based water discharges (Fig. 6),

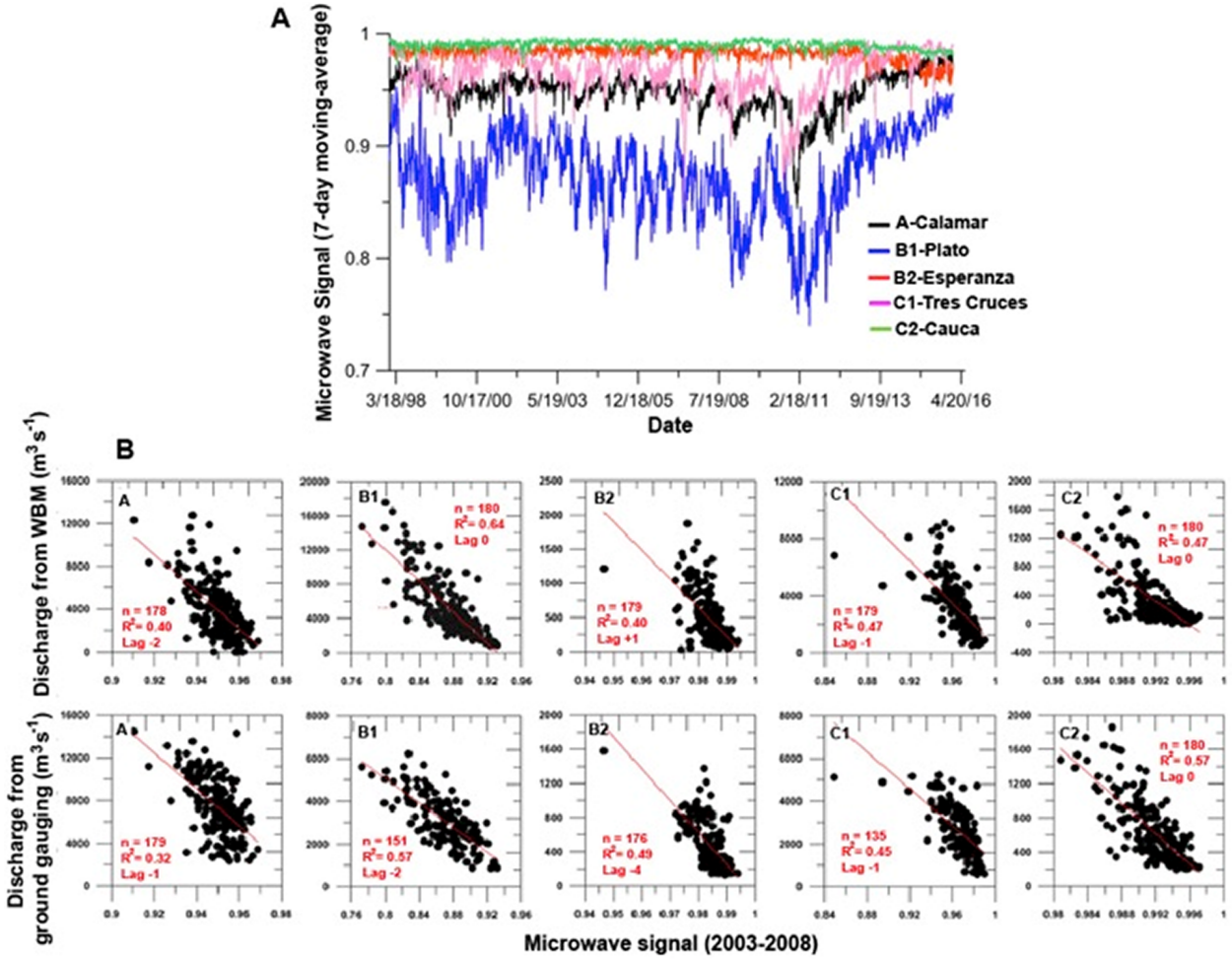

Fig. 7. (A) Timesseries of daily microwave satellite data developed by the Joint Research Center (JRC), Italy, at the satellite stations in the Magdalena River (Fig. 1B). (B) Regression fits between microwave signal and simulated discharges from WBM and ground models at the DFO satellite sites in the Magdalena River period (From Escobar et al., 2017; https://link.springer.com/chapter/10.1007/978-3-319-43744-6_1).

indicating that as water level rises, the water still has to pass through a more complex lagoon system before being detected. Thus, the observed phase-lag is possibly related to the hydrological dynamics of channel-floodplain connections. Nevertheless, stages of river-floodplain connection, visualized using daily MODIS satellite images, were superimposed to series of water level and satellite-based water discharge during La Niña, El Niño and neutral years (e.g., Fig. 3D-F and 5). According to the identified thresholds of river-lagoon connectivity (Fig. 6), percentages of connection time were estimated from frequency histograms of water level and satellite-based water discharge series (Fig. 5).

Main statistics of water level (m) and satellite-based water discharge ($m^3\ s^{-1}$) at Barbacoas lagoon and the Momposina depression floodplain, during periods of La Niña, El Niño and neutral years are shown in Table 2. Percentages of time of river-floodplain connectivity obtained by utilizing satellite-based discharges and gauging station water level are very similar, indicating that once connectivity thresholds are defined for each floodplain system, satellite-based timeseries are a good indicator of river floodplain connectivity. In addition, annual flood maps developed by DFO at Barbacoas lagoon and the Momposina depression show that annual flood frequencies (%) observed in channels next to the floodplains (Fig. 9) are in agreement with estimated times of connectivity (%) shown in Table 2. However, differences between flood frequencies (%) (Fig. 9) and time of connectivity (%) (Table 2), observed during La Niña years, may be due to the fact that DFO flood frequency maps do not include the strongest La Niña event on record in 2010–2011 or could be biased by clouds as flood frequency results are derived from MODIS optical bands.

5. Discussion and conclusions

For this study, we analyzed timeseries of satellite-based and ground-based gauging water discharge only for the period 1998–2016 (Fig. 1C and 8) as more recent ground-based data was not yet released at the time of the study. Nevertheless, satellite-based daily river discharges in near-real-time for the studied sites are updated and made available through the Dartmouth Flood Observatory River Watch portal (http://floodobservatory.colorado.edu/DischargeAccess.html).

River discharge estimated at ground-based gauging stations is well simulated by satellite-based water discharges, especially at the floodplain stations such as Calamar (A), Plato (B1), and Tres Cruces (C1), where the satellite signal properly represents the natural variability of river flow along the Magdalena floodplains (Figs. 1C and 8).

In addition, good correlations between DFO satellite data and ground-based results were observed once lags of one or two months were applied to river discharges with respect to the satellite signal (Table 1 and Fig. 7B). Water discharges at gauging stations are obtained from stage height variations while satellite river flow measurements are based on width variations of the water surface extension.

The existence of consistent lag times between station data and the satellite method requires discussion (Table 1 and Fig. 7B). As noted, ground stations track river discharge changes by river level (stage) at

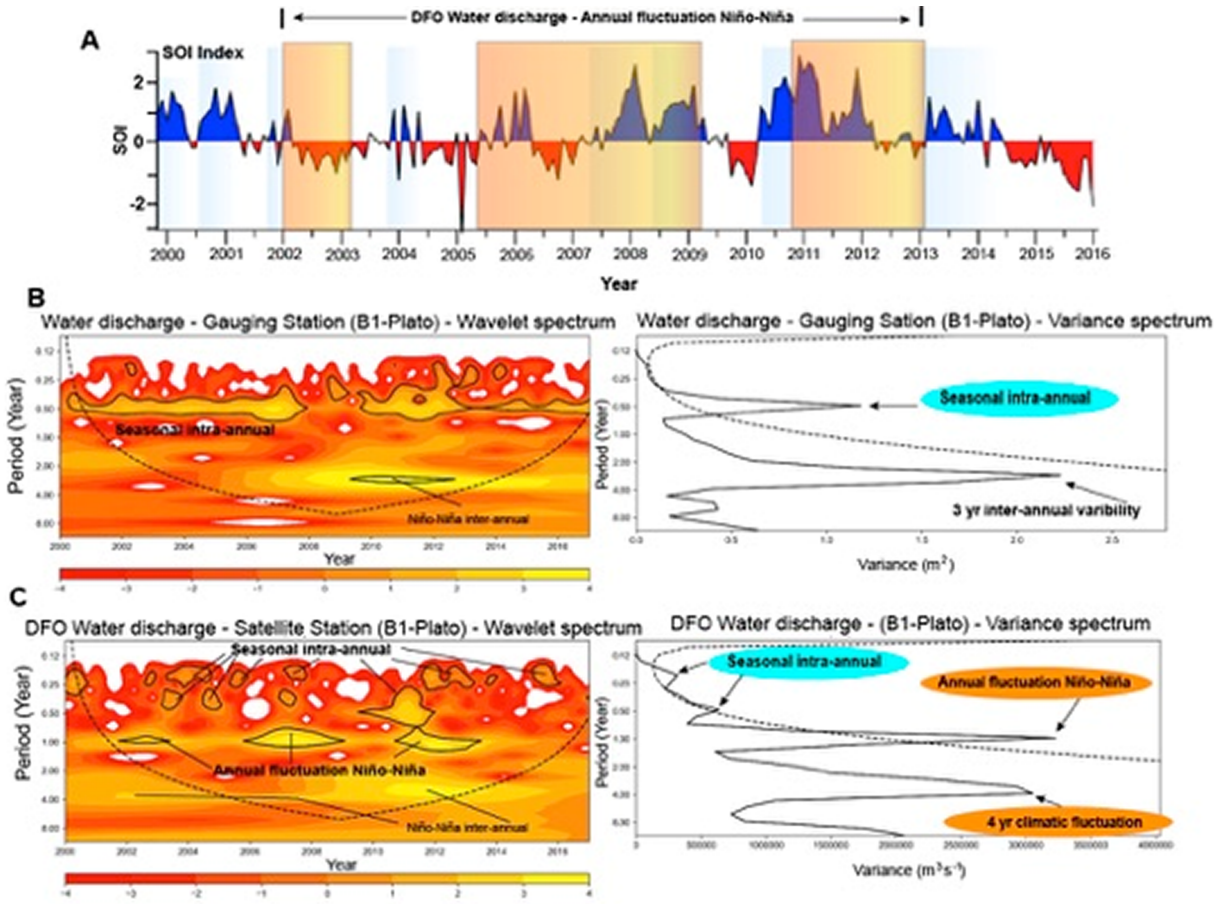

Fig. 8. (A) The Southern Oscillation Index (SOI) showing the period in which the DFO satellite-based water discharge series capture El Niño-La Niña inter-annual variability. (B) Wavelet spectrums of ground-based gauged water discharge and satellite-based water discharge at the Momposina depression floodplain for the period 2000–2016. In the variance spectrums (right B and C) it is shown how well DFO captures the annual seasonality and 4-year inter-annual variability due to El Niño-La Niña cycle compared to ground-based gauged water discharges.

one location. The local relation of actual discharge to stage may change over time with channel bathymetric/morphology changes at the station: stations are in fact often preferentially located to minimize such interference. Also, according to the flow continuity equation ($Q = w*d*v$), stage and flow area both track only particular aspects of discharge: in principle, velocity may be increasing as discharge increases (and a deformable river bed is eroded); stage could remain constant as discharge increases; hysteresis of stage/discharge relations is in fact common (Meade, 1988). Flow area changes for 10 km reaches along large rivers, on the other hand, may exhibit lag times to incoming increasing discharge and also be relatively less affected by local channel erosion or deposition. Thus, while stage normally increases with higher discharge, the water requires time to progressively inundate the local floodplain and change the satellite signal, even if overbank flow is being achieved. Any complex flow dynamics may be integrated, in this way, into the "bulk" water surface area measured each day and as monitored by the sensor: but with some lag time as compared to river stage at one station. This approach thus offers an entirely new way to monitor river flow changes, and advantages and constraints that complement those posed by traditional ground gauging stations.

The analysis of lag times between water level data and satellite observations also requires the consideration of the seasonal hysteresis between floodplain lakes water extent and floodplain water level (Rudorff et al., 2014; Park and Latrubesse, 2017). This hysteresis results in dissonance in the lake local-recharge and disconnection thresholds. In general, the water extent slowly increases during the early stages of rising water level and decreases during early falling water level. In rising levels, water extent starts to increase at certain water level thresholds. This shows that the water extent is not sensitive to the river stage changes when the maximum water extent in floodplain is reached. However, water volume in the floodplain is still increasing during this period, as the water from the main channel is continuously being transferred to the floodplain. In general, even before the river bankfull stage (i.e. river stage when it starts to overflow), the floodplain is already saturated and fully covered by water. In the Amazon, for example, water level still increases more than 3 m without changing the water extent (Park and Latrubesse, 2017).

Here, we show the performance of satellite-based discharges to assess preliminary threshold discharges (so stage) of river-floodplain connectivity (Table 2). At downstream stations, discharge variability and magnitudes are well captured by DFO water discharge series (Fig. 1C and 8; Table 1). The applicability of satellite-based discharges is limited at locations on confined channels without floodplains. In contrast, the changes of water surface area in braided, meandering or anastomosing channels are well correlated to satellite discharge. It is well known that the discharge volume of a given river channel cross-section is exceeded during peak discharge events. In anabranching channels of the Momposina depression floodplain, characterized by lateral connectivity to floodplains (a condition not necessarily related to overbank flows), effective water surface area can maintain a more constant relation to discharge over longer time periods (Smith, 1997; Smith et al., 1995; 1996). Thus, for these conditions, the satellite signal measures more accurately the river discharge magnitude. Our results clearly demonstrate the quality of satellite-based water discharges along stations in the floodplains of the Magdalena River (Fig. 1C, Table 1).

Table 2
Main statistics of water level (m) and satellite-based water discharge at Barbacoas lagoon (gray) and Momposina depression floodplain during 2000–2017, including periods of La Niña, El Niño and neutral years. Percentages of time of river-floodplain connectivity are indicated as well.

Barbacoas Lagoon					*Momposina Depression Floodplain*			
Gauged Water Level	Period 2000-2017	Niña years	Niño years	Neutral years 2012-2013	Period 2000-2017	Niña years	Niño years	Neutral year 2012-2013
Data points (n)	6283	1690	1521	366	…..	274	367	170
Mean (m)	3,44	3,72	3,16	3,20	…..	12,03	8,04	7,70
Max (m)	5,95	5,49	5,95	4,75	…..	15,10	10,70	10,0
Min (m)	1,06	1,06	1,55	2,13	…..	8,62	6,35	5,21
Mode (m)	3,20	3,80	2,80	3,0	…..	13,5	7,2-10,2	6,2-9,8
Standard dev.	0,68	0,67	0,67	0,49	…..	2,06	1,20	1,54
Coef. variation	0,20	0,17	0,21	0,15	…..	0,17	0,14	0,20
Connectivity threshold (m)	4,20	4,20	4,20	4,20	…..	12,0	12,0	12,0
% Time of connectivity	**17%**	**29%**	**11%**	**5%**	…..	**58%**	**8,6%**	**1,13%**
DFO Water Discharge	Period 2000-2017	Niña years	Niño years	Neutral years 2012-2013	2000-2017	Niña years	Niño years	Neutral year 2012-2013
Data points (n)	6533	1941	1522	366	6518	1941	1522	170
Mean ($m^3 s^{-1}$)	3276	3588	3161	2773	5172	7483	4183	3431
Max ($m^3 s^{-1}$)	15085	10751	15085	8115	20118	20118	16908	9500
Min ($m^3 s^{-1}$)	123	509	577	90	57	92	57	1580
Mode ($m^3 s^{-1}$)	3000	3000	3000	2500	2000	6000	1000	3500
Standard dev.	1374	1360	1320	1252	3306	3718	2981	1110
Coef. variation	0,42	0,37	0,41	0,45	0,64	0,50	0,71	0,32
Connectivity threshold ($m^3 s^{-1}$)	5000	5000	5000	5500	10000	10000	10000	9000
% Time of connectivity	**21%**	**32%**	**14%**	**3.8%**	**13%**	**38%**	**5%**	**1,7%**

Note: At Barbacoas lagoon, numbers of data points (n) of ground-based gauged water level are not the same as the satellite-based observations of water discharge due to unavailability of ground-based gauged data during some periods. At the Momposina depression floodplain gauging station, water level data is available since November 2010. Thus, for this site, water level thresholds are defined based on statistics during neutral, El Niño, and La Niña years for the period 2010–2016.

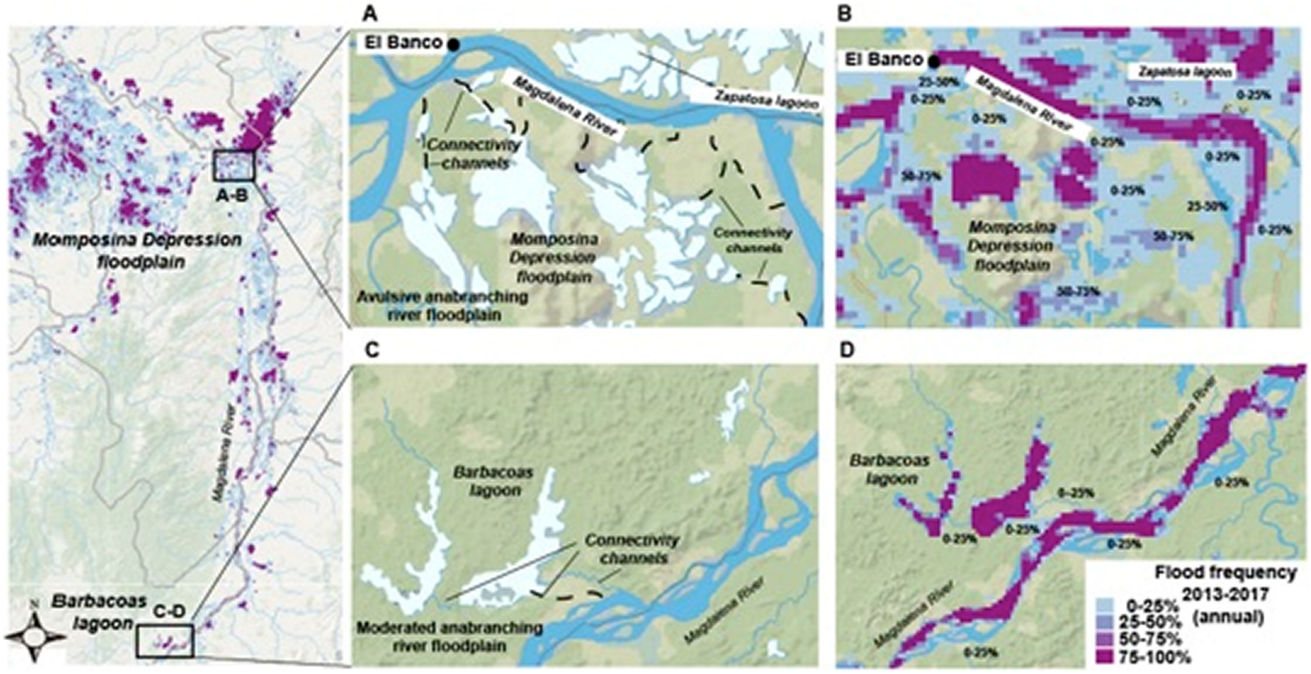

Fig. 9. Remote sensed flood frequency maps at Barbacoas and Momposina depression floodplains (Fig. 1B) during the period 2013–2017, showing percentages of annual flood at each lagoon and their connectivity channels. Observed times of river-floodplain connection by examining frequency distributions of water level and DFO water discharge (Table 2) are of the same magnitude as flood frequencies shown in these maps.

In large anabranching rivers (i.e., Amazon River and the Momposina depression floodplain in the Magdalena River), hydro-geomorphology has to be considered as part of the analysis of hydrological connectivity processes (Drago et al., 2008; Lininger and Latrubesse, 2016; Stevaux et al., 2013). In addition to the wide spectrum of the water stage variability, connectivity processes are affected by the complexity of the floodplain hydro-geomorphologic processes, including channelized flow routing paths, overbank diffusion, and local recharge (Latrubesse, 2012; Park and Latrubesse, 2017). Therefore, specific studies have to be carried out, in reach by reach, to calibrate individual thresholds of hydrological connection-disconnection levels and flood routing paths that are dependent on the internal geomorphic variability of the floodplain (Park and Latrubesse, 2017). In the Magdalena floodplains further in-situ studies should be conducted in order to understand how the flood pulse is related to the lateral connectivity and the specific river stage thresholds for the hydrologycal connectivity of different

geomorphic units.

The capabilities of using satellite data to estimate magnitudes of water discharge during high flow conditions are also shown in this study. During La Niña positive pulses between 2008 and 2011 (Fig. 1C and 8), peak discharges along the Magdalena floodplains were well simulated by the satellite signal, most likely even more precisely than those measured at hydrological gauging stations.

In countries like Colombia, many rivers are not gauged because of the intense civil conflict and the difficulty to access remote and undeveloped river regions. Thus, remote sensing approaches are a useful tool to monitor water discharge and floodplain responses to human induced activities and climate change. According to Sierra et al. (2017), plans to develop monitoring systems that combine satellite data with in-situ measurements are currently being considered by environmental authorities. However, the slow political reaction to establish these monitoring programs does not allow to record current environmental changes in Colombian drainage basins. Scientists can engage policy makers and stake holders such that hydrological monitoring is relevant to decision-making processes, and so environmental policies can be based on the best available scientific data (Salazar et al., 2018). In this study, we show that satellite-derived water discharges are reliable data for river planners and scientists, and also, the support information for exploring hydrological and ecological questions concerning floodplain services, water supply, and flood hazard mitigation.

Declaration of Competing Interest

The authors declare that they have no known competing financial interests or personal relationships that could have appeared to influence the work reported in this paper.

Acknowledgments

This work was supported by the US National Academy of Sciences under the funded PEER project (grant number 70). This paper highlights the collaboration between EAFIT University-Colombia and the DFO – Flood Observatory at the University of Colorado. We also thank the U.S. National Science Foundation, the European Commission's Joint Research Centre (JRC), and NASA through the project Near Real Time Flood Inundation Prediction and Mapping (NNX14AQ44G-NASA). Special thanks to USAID-Colombia for its support on implementing this PEER project in Colombia.

References

Alsdorf, D.E., Rodriguez, E., Lettenmaier, D.P., 2007. Measuring surface water from space. Rev. Geophys. 45, RG2002.
Barletta, M., Jaureguizar, A.J., Baigun, C., Fontoura, N.F., Agostinho, A.A., et al., 2010. Fish and aquatic habitat conservation in South America: a continental overview with emphasis on Neotropical systems. J. Fish Biol. 76, 2118–2176.
Bjerklie, D.M., Dingman, S.L., Vorosmarty, C.J., Bolster, C.H., Congalton, R.G., 2003. Evaluating the potential for measuring river discharge from space. J. Hydrol. 278, 17–38.
Bjerklie, D.M., Moller, D., Smith, L.C., Dingman, S.L., 2005. Estimating discharge in rivers using remotely sensed hydraulic information. J. Hydrol. 309, 191–209.
Brakenridge, G.R., Cohen, S., Kettner, A.J., De Groeve, T., Nghiem, S.V., Syvitski, J.P.M., Fekete, B.M., 2012. Calibration of satellite measurements of river discharge using a global hydrology model. J. Hydrol. 475, 123–136.
Brakenridge, G.R., Nghiem, S.V., Anderson, E., Mic, R., 2007. Orbital microwave measurement of river discharge and ice status. Water Resour. Res. 43, 1–16.
Brakenridge, G.R., Nghiem, S. V., Anderson, E., Chien, S., 2005. Space-Based Measurement of River Runoff. EOS, Transations, Am. Geophys. Union 86, 185-192.
Brakenridge, G.R., Knox, J.C., Paylor, E.D., Magilligan, F.J., 1994. Radar remote sensing aids study of the Great Flood of 1993. Eos, Trans. Am. Geophys. Union 75, 521-527.
Bray, W., 2006. Searching for environmental stress: climatic and anthropogenic influences on the landscape of Colombia. In: Stahl, P.W. (Ed.), Archaeology in the lowland American Tropics: Current Analytical Methods and Applications. Cambridge University Press, New York, pp. 96–113.
Colin, J.G., Smith, L.C., 2014. Toward global mapping of river discharge using satellite images and at-many-stations hydraulic geometry. Proc. Natl. Acad. Sci, U.S.A. 11, 4788–4791.
De Groeve, T., Brakenridge, G.R., Paris, S., 2015. Global Flood Detection System Data Product Specifications. JRC Technical Report. Available at http://www.gdacs.org/flooddetection/Download/Technical_Note_GFDS_Data_Products_v1.pdf.
De Groeve, T., Kugler, Z., Brakenridge, G.R., 2007. Near Real-time Flood Alerting for the Global Disaster Alert and Coordination System. Proc. ISCRAM 33-40.
Drago, E.C., Paira, A.R., Wantzen, K.M., 2008. Channel-floodplain geomorphology and connectivity of the Lower Paraguay hydrosystem. Ecohydrol. Hydrobiol. 8, 31–48.
Etter, A., McAlpine, C., Phinn, S., Pullar, D., Possingham, H., 2006a. Unplanned land clearing of Colombian rainforests: spreading like disease? Landsc. Urban Plan. 77, 240–254.
Etter, A., McAlpine, C., Wilson, K., Phinn, S., Possingham, H., 2006b. Regional patterns of agricultural land and deforestation in Colombia. Agric. Ecosyst. Environ. 114, 369–386.
Etter, A., McAlpine, C., Possingham, H., 2008. Historical patterns and drivers of landscape change in Colombia since 1500: a regionalized spatial approach. Ann. Assoc. Am. Geogr. 98, 2–23.
Escobar, C.R., Restrepo, J.D., Brakenridge, G.R., Kettner, A.J., 2017. Satellite-Based Estimation of Water Discharge and Runoff in the Magdalena River, Northern Andes of Colombia. In: Lakshmi V. (eds) Remote Sensing of Hydrological Extremes. Springer Remote Sensing/Photogrammetry. Springer, Cham, https://link.springer.com/chapter/10.1007/978-3-319-43744-6_1.
Gleason, C.J., Smith, L.C., 2014. Toward global mapping of river discharge using satellite images and at-many-stations hydraulic geometry. Proc. Natl. Acad. Sci. U.S.A. 11, 4788–4791.
Hoyos, N., Escobar, J., Restrepo, J.C., Arango, A.M., Ortiz, J.C., 2013. Impact of the 2010–2011 La Niña phenomenon in Colombia, South America: The human toll of an extreme weather event. Appl. Geogr. 39, 16–25.
Jaramillo-Villa, U., Cortes-Duque, J., Flórez, C., 2015. Colombia anfibia. Un país de humedales. Vol. I and Vol. II. (Instituto de Investigación de Recursos Hidrobiológicos Alexander von Humboldt). http://www.humboldt.org.co/es/estado-de-los-recursos-naturales/item/802-colombiaanfibiav1.
Kettner, A.J., Restrepo, J.D., Syvitski, J.P.M., 2010. A Spatial Simulation Experiment to Replicate Fluvial Sediment Fluxes within the Magdalena River Basin, Colombia. J. Geol. 118, 363–379.
Koblinsky, C.J., Clarke, R.T., Brenner, A.C., Frey, H., 1993. Measurement of river level variations with satellite altimetry. Water Resour. Res. 29, 1839–1848.
Kugler, Z., Nghiem, S.V., Brakenridge, G.R., 2019. L-band passive microwave data from SMOS for river gauging observations in tropical climates. Remote Sens. 11, 835.
Lakshmi, V., Fayne, J., Bolten, J., 2018. A comparative study of available water in the major river basins of the world. J. Hydrol. 567, 510–532.
Latrubesse, E.M., 2012. Amazon Lakes. In L. Bengtsson, R. Herschy, & R. Fairbridge (Eds.), Lakes and Reservoirs, pp. 13-26. Springer Verlag.
Latrubesse, E.M., 2015. Large rivers, megafans and other Quaternary avulsive fluvial systems: a potential who's who in the geological record. Earth-Sci. Rev. 146, 1–30.
Lininger, K.B., Latrubesse, E.M., 2016. Flooding hydrology and peak discharge attenuation along the middle Araguaia River in central Brazil. CATENA 143, 90–101.
Meade, R.H., 1988. Movement and storage of sediment in river systems, in: A. Lerman, A., Meybeck, M. (Eds.), Physical and chemical weathering in geochemical cycles. Kluwer, pp.165-179.
Milliman, J.D., Farnsworth, K., 2011. River Discharge to the Coastal Ocean – A Global Synthesis, first ed. Cambridge University Press, Cambridge.
Park, E., Latrubesse, E.M., 2017. The hydro-geomorphologic complexity of 1 the lower Amazon River floodplain and hydrological connectivity assessed by remote sensing and field control. Remote Sens. Environ. 198, 321–332.
Plazas, C., Falchetti, A.M., Van der Hammen, T., Botero, P.J., 1988. Cambios ambientales y desarrollo cultural en el Bajo Río San Jorge. Bol. Mus. Oro Banco Repúb. 20, 58–59.
Poveda, G., Jaramillo, A., Gil, M., Quiceno, N., Mantilla, R., 2001. Seasonality in ENSO related precipitation, river discharges, soil moisture, and vegetation index (NDVI) in Colombia. Water Resour. Res. 37, 2169–2178.
Poveda, G., Waylen, P.R., Pulwarty, R.S., 2006. Annual and inter-annual variability of the present climate in northern South America and southern Mesoamerica. Palaeogeogr. Palaeoclimatol. Palaeoecol. 234, 3–27.
Restrepo, J.D., Escobar, H.A., 2018. Sediment load trends in the Magdalena River basin (1980–2010): anthropogenic and climate-induced causes. Geomorphology 302, 76–91.
Restrepo, J.D., Escobar, R., Tosic, M., 2018. Fluvial fluxes from the Magdalena River into Cartagena Bay, Caribbean Colombia: trends, future scenarios, and connections with upstream human impacts. Geomorphology 302, 92–105.
Restrepo, J.D., Kettner, A., Syvitski, J.P.M., 2015. Recent deforestation causes rapid increase in river sediment load in the Colombian Andes. Anthropocene 10, 13–28.
Restrepo, J., Ortíz, J.C., Pierini, J., Schrottke, K., Maza, M., Otero, L., Aguirre, J., 2014. Freshwater discharge into the Caribbean Sea from the rivers of Northwestern South America (Colombia): magnitude, variability and recent changes. J. Hydrol. 509, 266–281.
Restrepo, J.D., Kjerfve, B., Restrepo, J.C., Hermelin, M., 2006. Factors controlling sediment yield from a major South American Drainage Basin: The Magdalena River, Colombia. Journal of Hydrology 316, 213–232.
Restrepo, J.D., Syvitski, J.P.M., 2006. Assessing the effect of natural controls and land use change on sediment yield in a major Andean River: The Magdalena Drainage Basin, Colombia. Ambio 35, 44–53.
Restrepo, J.D., Kjerfve, B., 2000. Magdalena River: Interannual variability (1975–1995) and revised water discharge and sediment load estimates. J. Hydrol. 235, 137–149.
Rudorff, C.M., Melack, J.M., Bates, P.D., 2014. Flooding dynamics on the lower Amazon floodplain: hydraulic controls on water elevation, inundation extent, and river-floodplain discharge. Water Resour. Res. 50, 619–634.
Salazar, A., et al., 2018. The ecology of peace: preparing Colombia for new political and

planetary climates. Front. Ecol. Environ. 16, 1–7.
Sierra, C.A., Mahecha, M., Poveda, G., et al., 2017. Monitoring ecological change during rapid socio-economic and political transitions: Colombian eco- systems in the post-conflict era. Environ. Sci. Policy 76, 40–49.
Smith, D.G., 1986. Anastomosing river deposits, sedimentation rates and basin subsidence, Magdalena River, northwestern Colombia, South America. Sedimentol. Geol. 46, 177–196.
Smith, L.C., 1997. Satellite remote sensing of river inundation area, stage, and discharge: a review. Hydrol. Process. 11, 1427–1439. https://doi.org/10.1002/(sici)1099-1085(199708)11:10<1427::aid-hyp473>3.0.co;2-s.
Smith, L.C., Isacks, B., Bloom, A., 1996. Estimation of discharge from three braided rivers using synthetic aperture radar satellite imagery: Potential application to ungauged basins. Water Resour. Res. 32, 2021–2034.
Smith, L.C., Isacks, B., Forster, R.R., Bloom, A., Preuss, I., 1995. Estimation of discharge from braided glacial rivers using ERS1 synthetic aperture radar: first results. Water Resour. Res. 31, 1325–1329.
Stevaux, J.C., Corradini, F.A., Aquino, S., 2013. Connectivity processes and riparian vegetation of the upper Paraná River, Brazil. J. South American Earth Sciences 46, 113–121.
The Nature Conservancy, Fundación Alma, Fundación Humedales and Autoridad Nacional de Pesca, 2016. Estado de las planicies inundables y el recurso pesquero en la macrocuenca Magdalena-Cauca y propuesta para su manejo integrado. (The Nature Conservancy. Bogotá, Colombia. Bogotá, Colombia). Available at https://www.mundotnc.org/nuestro-trabajo/donde-trabajamos/america/colombia/estado-y-propuesta-para-el-manejo-de-las-planicies-inundables-y-el-recurso-p.xml.
Torrence, C., Compo, G., 1998. A practical guide to wavelet analysis. Bull. Am. Meteorol. Soc. 79, 61–78.
Van Dijk, A.I.J.M., Brakenridge, G.R., Kettner, A.J., Beck, H.E., De Groeve, T., Schellekens, J., 2016. River gauging at global scale using optical and passive microwave remote sensing. Water Resour. Res. 52, 6404–6418.
Walschburger, T., Angarita, H., Delgado, J., 2015. Hacia una gestión integral de las planicies inundables en la cuenca del Magdalena-Cauca. In: Rodríguez Becerra, M. (Ed.), ¿Para dónde va el río Magdalena? Riesgos sociales, ambientales y económicos del proyecto de navegabilidad. Foro Nacional Ambiental-FESCOL, Bogotá, pp. 145–168.